People's Democratic Republic of Algeria
Ministry of Higher Education and Scientific Research
A. Mira University of Bejaia

جامعة بجاية
Tasdawit n Bgayet
Université de Béjaïa

Faculty of Exact Sciences
Department of Physics

Master's Thesis

Presented by

Ms. AZIB Nessrine

Specialty: Physics of materials

Theme

Analysis of stress drops associated with the heterogeneous plastic deformation in the Al-3.2%Mg alloy

July 12, 2022

Members of the jury :

GHARBI	*Abdelhakim*	*Professor*	*Chair*
BOUFALA	*Khaled*	*LCA*	*Examiner*
AIT AMOKHTAR	*Hakim*	*Professor*	*Supervisor*

Academic year: 2021/2022

“Crystals are like humans …
It is the defects in them which tend to make them interesting! ”

Frederick Charles Frank

(English physicist, 1911- 1998)

“Crystals reveal their hidden structures only when broken”

Sigmund Freud

(Austrian neurologist 1856-1939)

Acknowledgements

First of all, it is my pleasure to testify my sincere gratitude and my deep sense of respect to my honorable teacher and educational supervisor, Mr. ***Hakim Ait Amokhtar****, for giving me such a golden opportunity to work on this wonderful project on Analysis of stress drops associated with the heterogeneous plastic deformation in the Al-Mg alloy, for their relevant recommendations, for the valuable words, advice, motivation and ongoing monitoring throughout the development of this research. I would like to express my gratefulness in terms of my high consideration for their passion and enthusiasm for studies. I would like to thank Mr.* ***Abdelhakim Gharbi*** *for giving me the honor of presiding over the jury for my graduation and Mr.* ***Khaled Boufala*** *for being interested in this work and for agreeing to evaluate it.*

Last but not least, all thanks and appreciation to all those who helped to the good conduct of this thesis.

Dedication

For me, myself and I

For the memory of my precious grandmother

For my dearest father and mother

For my two best brothers Habib and AbdRaouf

For my blood sister Wided

For my best friends Salma, the three Rymas, Assia, Aldja

For my family, uncles and aunts especially Samia, Yamina, Saida

For my dearest cousin Nadia

For all my friends

For the entire physical promotion

For all those I love and those who love me

Nessrine

Table of contents

Chapter II: Dynamic strain aging and plastic instabilities in metals

Chapter III: Analysis of stress drops associated to jerky flow in the Al-3.2%Mg alloy

List of figures

List of tables

General introduction

General introduction

Around two thirds of the elements in the periodic table are metals, although for engineering purposes we're particularly interested in just a handful of them. Aluminium is commonly used because its alloys have high strength-to-weight ratio. It has a relatively low melting temperature (~660°C), which makes it easier to process and use for casting, and it's inexpensive. Other important metals include Magnesium, Iron, Titanium, Copper, and Nickel. In metallic materials, imperfections and crystalline defects are omnipresent. During structural transitions, these defects can interact and proliferate. Therefore they play a very crucial role in determining the physical, mechanical and chemical properties of materials. This is the case with plastic deformation, which is mainly determined by the crystal glide of dislocations. To be able to use these metals effectively, it's essential to understand how they are structured at the atomic level.

Plastic deformation is discontinuous and heterogeneous at the microscopic scale, despite its homogeneous and continuous characteristics at the macroscopic scale. However, the main difficulty in materials science lies in the transition from the individual behaviour of a dislocation to mechanical properties of materials at the macroscopic level. The mechanical behaviour of metallic materials is usually characterized by average macroscopic values: Young's modulus, elastic limit, yield strength… etc.

In the present work, after a review of the plastic deformation of metallic materials, we study the plastic deformation of an aluminium-magnesium alloy at the material macroscopic level using uni-axial tensile tests. In addition to an introduction and a conclusion, this brief is structured in three chapters:

- The first chapter is a bibliographical synthesis on crystalline defects, plastic deformation and mechanical behaviour of metallic materials, in particular dislocations and their role in deformation.
- In the second chapter, we give a general idea about plastic instabilities, and then we put our interest in dynamic strain aging (DSA) and the Portevin-Le Chatelier effect.
- The third chapter will be devoted to the experimental characterization of the Portevin-Le Chatelier effect in the Al-3.2%Mg alloy at room temperature.

Chapter I

Plasticity of metallic materials

Chapter I

Plasticity of metallic materials

I.1.Introduction

Plastic deformation is an irreversible phenomenon that permanently changes the shape of materials. Therefore, understanding mechanisms that determine the plastic behavior of materials has important implications for the design and shaping of mechanical pieces according to well-defined criteria.

In metallic materials, plastic deformation is mainly produced by glide of dislocations. The later are an important class of defect. Metals and many important classes of non-metallic solids are crystalline, i.e. the constituent atoms are arranged in a pattern that repeats itself periodically in space. The actual arrangement of the atoms is described by the crystal structure. Metallic materials have a polycrystalline structure and their plasticity is more complex. It does not occur everywhere at once because the orientation of the grains is not almost favorable for dislocations motion.

In the following, before dislocations can be introduced, an elementary understanding of crystallinity is required. Therefore, we introduce the basic concepts of crystalline defects, plastic deformation, in particular dislocations and their role in deformation, and mechanical behavior of metallic materials.

I.2. Crystalline structure of metallic materials

I.2.1.Crystal structures

The crystal represents the state of matter most frequently encountered in materials, its structure is made of attaching atoms. The crystalline structure is an ordered array of atoms, ions or molecules. Generally, this structure stems from the intrinsic properties of the constituent particles to create symmetrical patterns. The repeating pattern of a small set of

atomic structures is called the unit cell of the structure. It is the building part of the crystal structure which explains the entire crystal structure and its symmetry with the atomic positions and their principal axes. The length, the edge of the principal axes, and the angle between the unit cells are called the lattice constants or lattice parameters [1-4].

The atoms of a pure metal can be thought of as identical perfect spheres; they are packed together closely and are arranged in a very regular grid. Because of this regular structure, metal is what we call a crystalline material, and the grid in which the atoms are arranged is called the crystal lattice. Not all materials have a regular structure; in glass for example the atoms are arranged randomly, so it's an amorphous material[2, 3].

A basic concept in crystal structure is the unit cell. It is the smallest unit of volume, allowing identical units to be stacked to fill the entire space. By repeating the unit cell pattern over and over in all directions, the whole crystal lattice can be built. A cube is the simplest example of a unit cell [2,3].

The metals all crystallize in one of four basic structures: simple cubic (*SC*), body-centred cubic (*BCC*), hexagonal closest-packed (*HCP*), and face centred cubic (FCC).

I.2.1.1.Simple Cubic packing

This crystal structure corresponds to a cube with an atom on each corner (Fig.I.1-a). The simple cubic unit cell may also be called primitive cubic. Each sphere in this structure touches four identical spheres in the same plane. It also touches a sphere on the upper layer and a sphere on the lower layer(Figs.I.1-b and I.1-c). Each atom in this structure can form bands with its six nearest neighbors. The spheres occupy about 52 % of the volume[1].

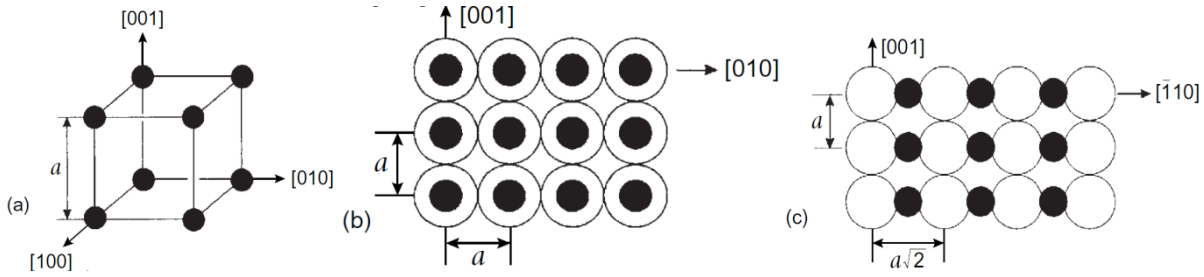

Figure I.1. Simple cubic structure: (a)unit cell, (b) arrangement of atoms in (100) layers, (c) arrangement of atoms in (110) layers [8].

I.2.1.2. BodyCentred Cubic (bcc) structure

In body-centred cubic structure, each atom has eight neighbors arranged at the corners of a cube(Fig. I.2). If atoms are of the same type and considered as spheres, they occupy 68 % of the volume. There are about 23 metals with the bcc arrangement [3].

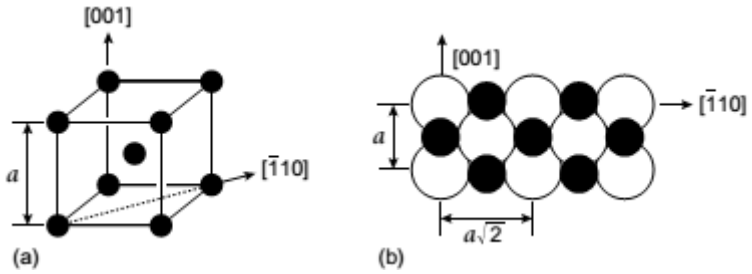

Figure I.2. Body-centred cubic structures: (a) unit cell, (b) arrangement of atoms in (110) layers [8].

I.2.1.3.Face Centred Cubic and Hexagonal Closest-packed structures

There are two possible arrangements with high compactness (Fig.I.3). The first layer, labelled A, has the atoms packed into a plane-triangular lattice in which every atom has six immediate neighbors. The second layer, labelled B, has the same plane-triangular structure; the atoms placed in the holes formed by the first layer. The first layer has two equivalent sets of holes, but the atoms of the second layer can occupy only one set. The third layer, labelled *C*, has the same structure, but there are two choices for selecting the holes that the atoms will occupy. The third layer can be placed over the atoms of the first layer, the sequence is *ABABAB*..., which is called the hexagonal closest packed (hcp)(Fig.I.4). Or the third layer goes over in C, and so there is a three-layer repetition *ABCABCABC*..., which is called the face centred cubic (fcc) (Fig.I.5). In the hcp and the fcc structures the spheres fill 74 % of the volume, which represents the closest possible packing of spheres. Each atom has 12 neighbors. There are about 32 metals that have the hcp and 26 with the fcc structures [1].

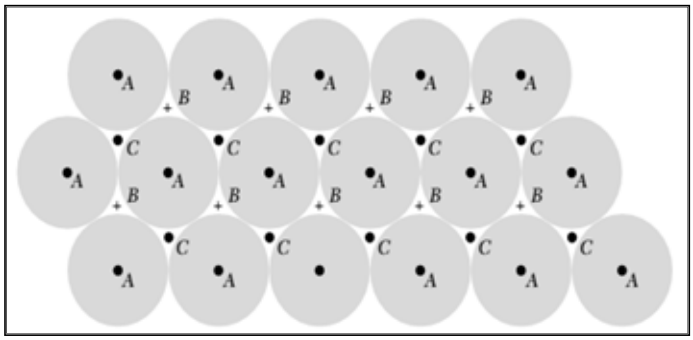

Figure I.3. Close-packed layer of spheres [1].

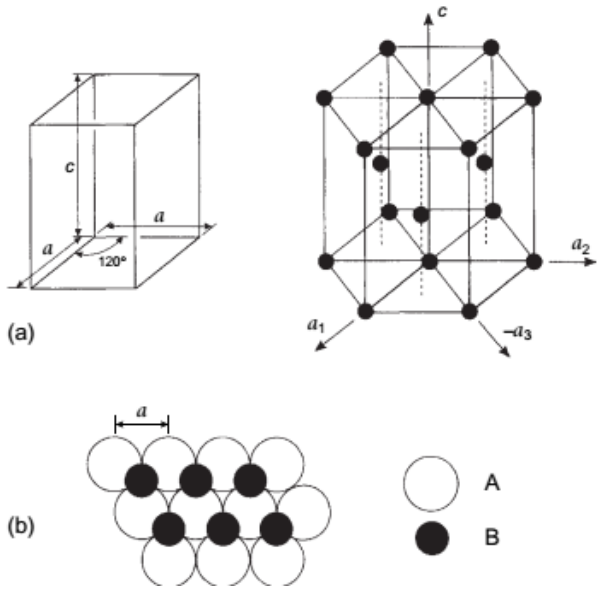

Figure I.4. Close-packed hexagonal structure: (a) the unit cell of the lattice and the hexagonal cell showing the arrangement of atoms, (b)ABAB...stacking sequence of the atomic planes perpendicular to the axis [8].

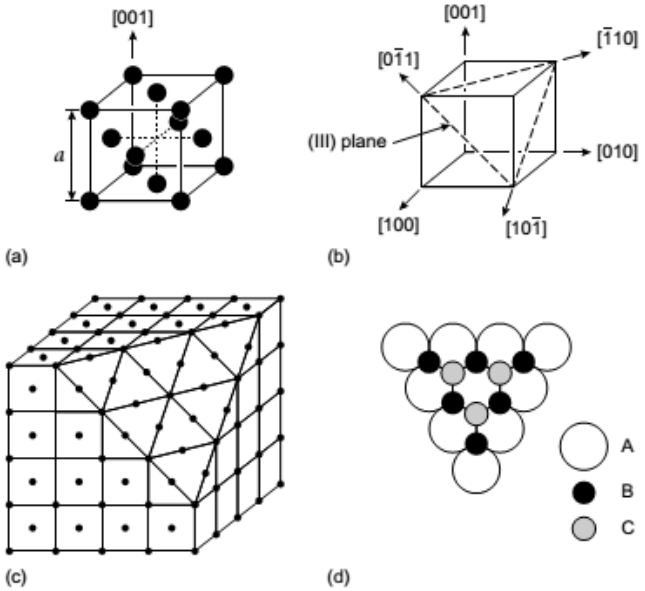

Figure I.5.Face-centred cubic structure: (a) unit cell, (b) principal directions, (c) arrangement of atoms in a (111) close-packed plane, (d) stacking sequence of {111} planes [8].

In reality, crystal lattices aren't perfect. They contain numerous defects which affect highly the proprieties of materials.

I.2.2. Crystal Defects

Crystal defects can be classified according to their geometrical forms and sizes.

I.2.2.1. Point defects

When a defect exists at the scale of an atom, we speak about a punctual defect. The presence of foreign atoms in the substrate produces the extrinsic defects, the wrong arrangement of certain atoms in the crystal lattice creates intrinsic defects, the absence of atoms is what we call vacancy defect. Point defects deform the lattice locally and create stress fields over a few interatomic distances around the defect. There are three main types of punctual defects[4,5,6].

a. Vacancy defect

A vacancy defect is created when an atom leaves its position in a lattice. Since the density of vacancy defects is high, atoms are able to migrate within the crystal lattice (Fig.I.6). This mechanism results from successive permutations of a hole and a neighbor atom that moves to occupy it. Consequently, the vacancies allow the diffusion of atoms in the crystal[4].

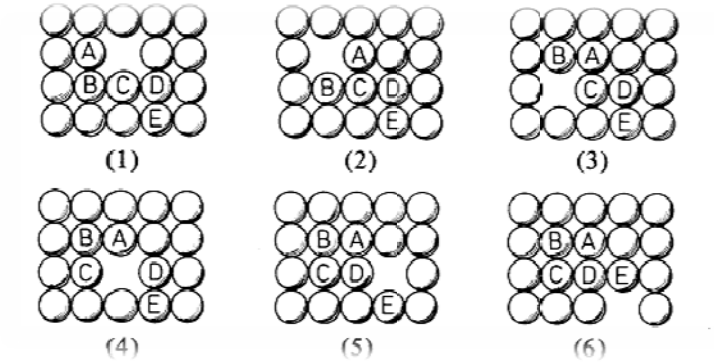

Figure I.6.Mechanism of vacancy migration of atoms in a crystal lattice: changing positions between atoms and holes (1 to 6)[5].

b. Interstitial defect

An interstitial defect occurs when a foreign small atom migrates into a space between atoms (interstice) in the lattice [4].

c. Substitutional defects

Substitutional defects correspond to certain atoms in the lattice substituted by impurities. The lattice is locally distorted around each foreign atom[4].

Vacancy, interstitial and substitutionnal defects are the elementary point defects; they affect a single location within the lattice. Their combinations and grouping over a few interatomic distances can form more complex defects (clusters, etc.).

I.2.2.2. Linear defects (Dislocations)

Linear defects, called dislocations, are disturbances (or discontinuities) of the crystalline structure along a line of atoms. There are two types of dislocations which are described in the following.

a. Edge dislocation

The first type of dislocation is an edge dislocation (Fig. I.7). Locally, asif the lattice contains an extra half plane of atoms. A linear disturbance is created along the bottom of the extra half plane, it corresponds to the edge dislocation (labeled ⊥).

When a stress is applied to the lattice, the atomic bands break and re-form, giving the impression that the extra half plane of atoms glides through the lattice. Dislocations motion will be discussed hereafter [4].

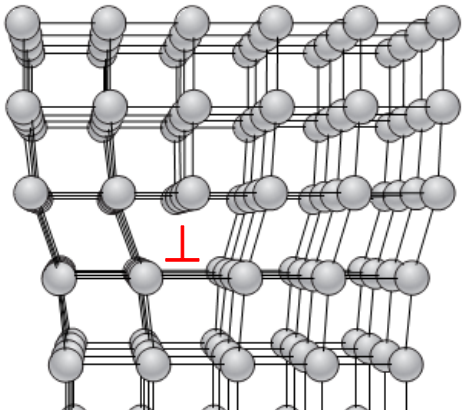

Figure I.7. Perspective view of the structure of an edge dislocation in a cubic lattice crystal[1].

b. Screw dislocation

Another type of dislocation is the screw dislocation, where a linear disturbance of atoms is created in a spiral form in the lattice structure (Fig.I.8). It gets its name because if we follow a path of atoms around the dislocation, it will spiral down through the lattice like the thread of a screw (Fig.I.8-c). When a shear stress is applied the atoms rearrange into a new stable configuration.

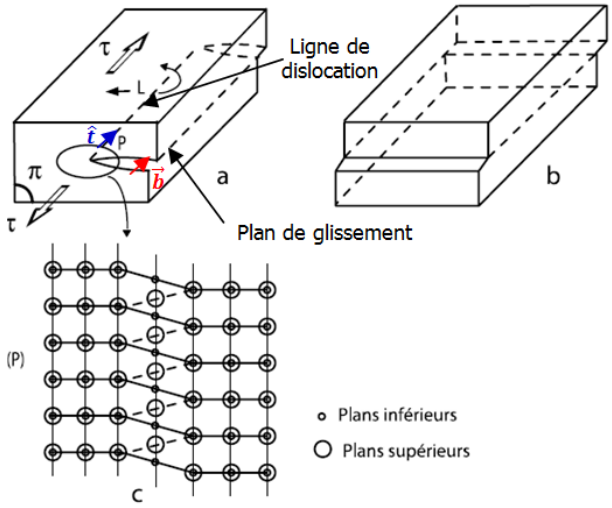

Figure I.8. (a) Schematic representation of a process of screw dislocation creation. (b) Step created by dislocation motion. (c) Atomic scale configuration of screw dislocation [4,5].

In fact, dislocations are a combination of edge and screw dislocations known as a mixed dislocation (Fig. I.9). Because dislocations move through the lattice by breaking and reforming atomic bands, the process is irreversible; when the applied shear stress is removed, the dislocations do not return to their original positions [4,5].

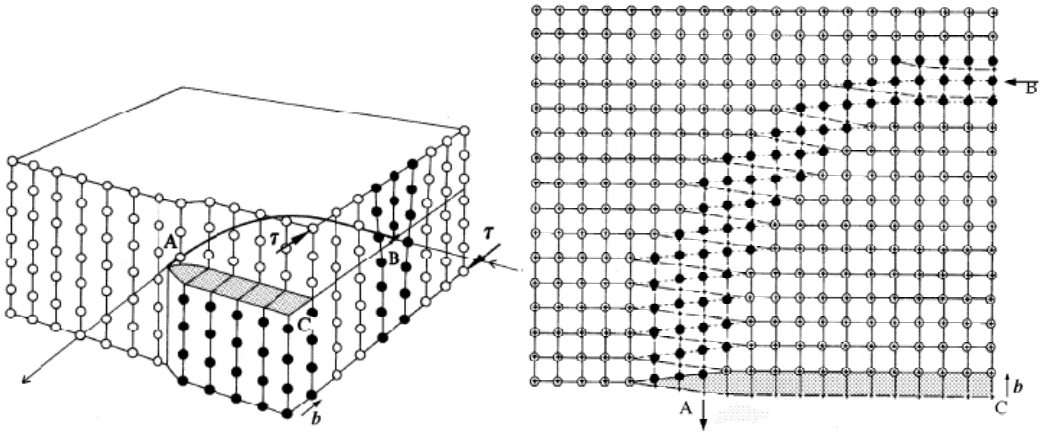

(a) (b)

Figure I.9.(a) Example of mixed dislocation with an edge dislocation component and a screw dislocation component. (b) Perpendicular view to ABC plane showing the transition from the pure screw dislocation (Point A) to the pure edge dislocation (Point B) [5].

I.2.2.2.1. Burgers vector

The Burgers vector $\vec{b}$is a characteristic parameter to describe a dislocation line. It is also known as slip vector, representing the direction and amount of slip associated with the dislocation [9]. $\vec{b}$is determined by the Burgers circuit (Fig. I.10).The direction of a dislocation

line is defined by the unit vector $\vec{t}$ that is tangent to it. The angle formed by both vectors $\vec{b}$ and $\vec{t}$ is the characteristic of a dislocation; in other words:

- For an edge dislocation: $\vec{b} \perp \vec{t}$
- For a screw dislocation: $\vec{b} // \vec{t}$
- For a mixed dislocation: the vectors are neither ⊥ nor //, there are two components of the burgers vector in each point of a mixed dislocation:
  - Edge component: $b_{edge} = b_{\perp} = b \sin\theta$, with $\theta = (\widehat{\vec{t}, \vec{b}})$.
  - Screw component: $b_{screw} = b_{//} = b \cos\theta$

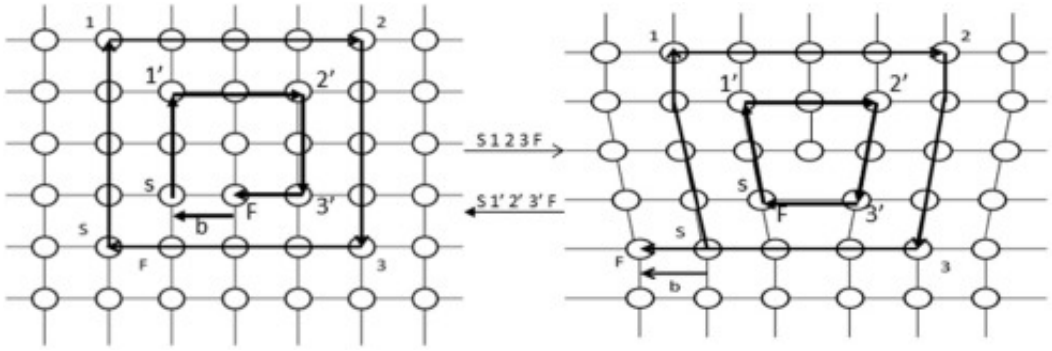

(a) (b)

Figure I.10.(a) Burgers circuit in a perfect crystal and (b) in presence of an edge dislocation[7].

I.2.2.2.2. Elastic properties of dislocations

A dislocation in material creates a local high distortion along its line, at a distance $r < r_0$. Where r_0 is the radius of the disturbance. In areas far from the dislocation core, at a distance $r > r_0$, the associated stress field can be determined by the elasticity theory. In order to define the stress state of a material at a given point under an external force, it is first crucial to know the components of the force applied perpendicular to all three sides of the cube surrounding that point (Fig.I.11).

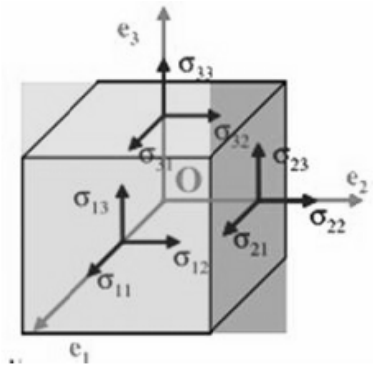

Figure I.11. Stress tensor components around an O point [17].

The stress tensor is:

$$\overline{\overline{\sigma}} = \begin{bmatrix} \sigma_{11} & \sigma_{12} & \sigma_{13} \\ \sigma_{21} & \sigma_{22} & \sigma_{23} \\ \sigma_{31} & \sigma_{32} & \sigma_{33} \end{bmatrix} \quad \text{(I.01)}$$

Similarly to the stress tensor, we can write the strain tensor:

$$\overline{\overline{\varepsilon}} = \begin{bmatrix} \varepsilon_{11} & \varepsilon_{12} & \varepsilon_{13} \\ \varepsilon_{21} & \varepsilon_{22} & \varepsilon_{23} \\ \varepsilon_{31} & \varepsilon_{32} & \varepsilon_{33} \end{bmatrix} \quad \text{(I.02)}$$

From these definitions we can deduce:

For an edge dislocation along z axis:

$$\overline{\overline{\varepsilon}} = \frac{b}{4\pi r^2} \begin{bmatrix} 0 & 0 & -y \\ 0 & 0 & x \\ -y & x & 0 \end{bmatrix} \quad \text{(I.03)}$$

$$\overline{\overline{\sigma}} = \frac{\mu b}{4\pi r^2} \begin{bmatrix} 0 & 0 & -y \\ 0 & 0 & x \\ -y & x & 0 \end{bmatrix} \quad \text{(I.04)}$$

μ: Theshear module and $r^2 = x^2 + y^2$.

For a screw dislocation along z axis:

$$\overline{\overline{\varepsilon}} = \begin{bmatrix} \varepsilon_{11} & \varepsilon_{12} & 0 \\ \varepsilon_{21} & \varepsilon_{22} & 0 \\ 0 & 0 & 0 \end{bmatrix} \quad \text{(I.05)}$$

$$\overline{\overline{\sigma}} = \begin{bmatrix} \sigma_{11} & \sigma_{12} & 0 \\ \sigma_{21} & \sigma_{22} & 0 \\ 0 & 0 & \sigma_{33} \end{bmatrix} \quad \text{(I.06)}$$

For a mixed dislocation, the strain and stress fields associated are overlays of the edge and screw components fields [4].

I.2.2.3. Surface and volume defects

Among surface defects, we can cite grains boundaries which affect highly material proprieties. Polycrystalline materials are made of a collection of grains (crystallites) which are randomly oriented in space (Fig.I.12). The grains are separated by grain boundaries, which constitute surface defects. The presence of grains hinders the movement of dislocations, so polycrystalline materials tend to be strength than materials composed of a single uniform crystal. Generally, the smaller the grain size is, the strength the material is [5].

When a defect spreads over a volume, it is called a volume defect. We can cite: precipitates, pores, ...

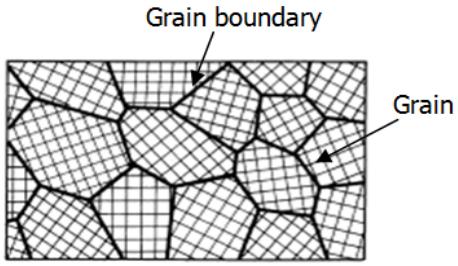

Figure I.12.Schematic representation of a polycristal microstructure[4].

I.3. Dislocation Mobility

I.3.1. Dislocation motion

Elastic deformation is caused by the stretching of atomic bands without their breaking. This stretching is reversible when the load is removed. In case of elastic deformation, there is no dislocations motion.

The displacement of a dislocation in a crystal results in the formation of a microscopic march, which permanently changes the shape of the crystal. This phenomenon is called plastic deformation. This change of the macroscopic form is due to the motion of a large number of dislocations at the atomic level [4,9].

Mainly, there are two basic types of dislocation motion:

- Glide or conservative motion occurs when the dislocation moves in the plane containing both its line and Burgers vector: such dislocation is glissile, one which doesn't is sessile.
- Climb or non-conservative motion occurs when the dislocation line moves up (or down) one atom spacing out of its original slip plane [8].

I.3.2. Slip system

The slip system is defined by the slip plane and the slip direction of a dislocation. Slip systems and their number depend on the nature of the crystal system.

The slip planes are the planes with the highest density of atoms and the slip direction corresponds to one of the shortest lattice translation vectors, in other words, the energy required to move the dislocation is the lowest [8]. Dislocations slip leads to the formation of steps on the crystal surface. These later are easily detected if the surface is carefully polished (Fig.I.13).

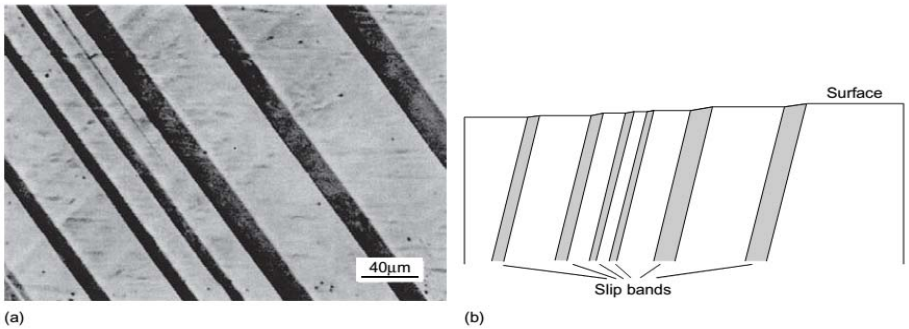

Figure I.13. (a) Slip bands on a single crystal of 3.25 per cent silicon iron. (b) Sketch of a section across the slip bands normal to surface shown in (a). Each band is made up of a large number of slip steps on closely spaced parallel slip planes [8].

I.3.3. Shear Stress

Slip of a dislocation requires a critical shear stress. Consider the crystal shown in Fig.I.14, which is deformed under tension with a force F applied along the axis of the cylinder. When the cross-sectional area is A, the tensile stress is parallel to F is:

$$\sigma = \frac{F}{A} \tag{I.07}$$

This force has a component $F\cos\lambda$ in the slip direction, where λ is the angle between F and the slip direction. This force acts on the slip surface of area $\frac{A}{\cos\varphi}$, where φ is the angle between F and the normal to the slip surface. So the shear stress τ, determined on the slip plane in the slip direction is:

$$\tau = \frac{F}{A}\, cos\, \varphi\, cos\, \lambda \tag{I.08}$$

The quantity $\cos\varphi\cos\lambda$ is known as the Schmid factor[8]. When F_c is the tensile force required to initiate slip, the corresponding value of shear stress τ_c is called the critical resolved shear stress for slip. For some crystals which deform on a single slip system, τ_c is independent of the crystal orientation [8].

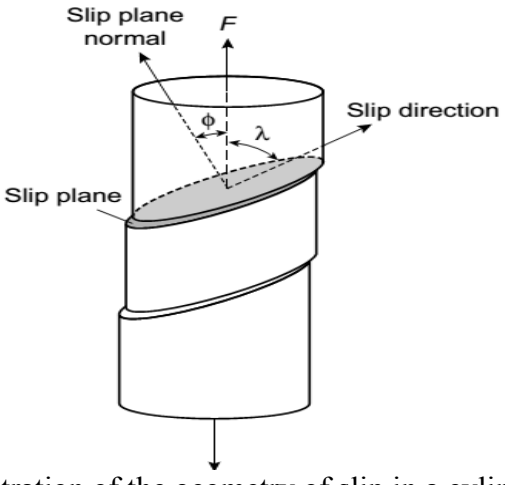

Figure I.14. Illustration of the geometry of slip in a cylindrical crystal [8].

I.3.4.Slip of edge dislocation

A dislocation slide under a critical shear stress $\tau = \tau_c$ creating a surface step of magnitude b (Fig.1.15, from (a) to (d)). In this case, the slip is a conservative mechanism because it does not require transport of material. It makes it possible to propagate the deformation under a low external stress [4].

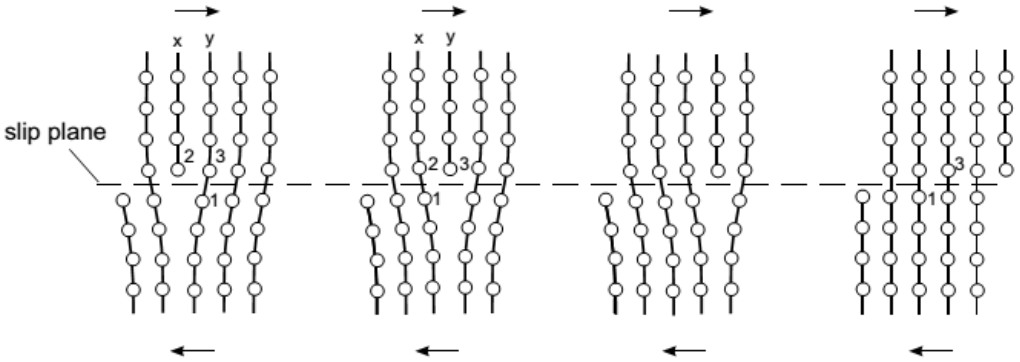

Figure I.15.Displacement of an edge dislocation under a shear stress. The arrows indicate the applied shear stress [8].

I.3.5. Cross Slip and Climb

Screw dislocations tend to move in certain crystallographic planes. Screw dislocation can slide from one plane to another non-parallel, this slip takes place when the screw dislocation is blocked by an obstacle, it's known as the cross slip (Fig.I.16) [4].

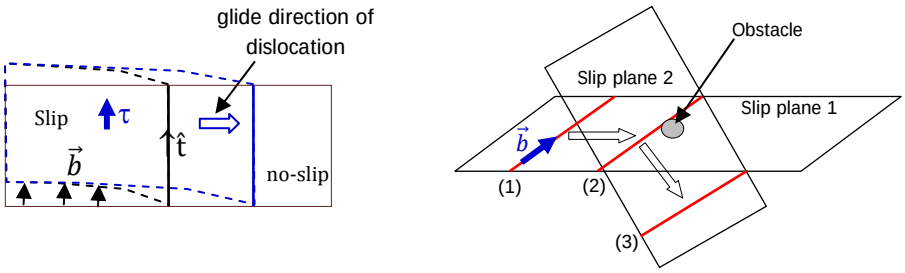

Figure I.16. Slip of screw dislocation under the effect of a shear stress[4].

An edge dislocation can move out of its slip plane towards an adjacent parallel plane by a climb (Fig.I.17).If the row of atoms A parallel to the plane in the figure bellow is removed, the dislocation line moves up one atom making a space of its original slip plane; this is called positive climb. If a row of atoms is introduced in the opposite way, the dislocation line moves down one atom, this is called negative climb [8].

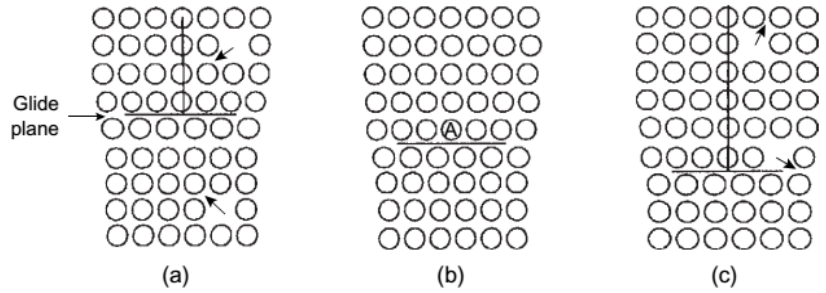

Figure I.17. Positive and negative climb of an edge dislocation [8].

I.4. Deformation tests of metallic materials

I.4.1.Types of mechanical testing

Mechanical testing can be used to analyze mechanical response of a material and to determine its mechanical properties. There are many different types of mechanical testing, the commonly used are:

a. Hardness Testing

Hardness test is used to measure the resistance of a surface to objects that are crushed under pressure or impact. Hardness test procedures are usually fast and easy to perform, the equipment required is relatively basic. The values measured depend upon the characteristics of the object measured which are: the tensile strength and the elastic limit, the elasticity modulus, the surface finish, and the homogeneity of the material[10, 12].

b. Tensile Testing

Tensile test is a destructive process that provides the stress-strain curve for materials as well as properties including yield stress, tensile stress, percentage elongation to failure, Young's modulus and ductility. It measures the force needed to break a specimen and the extent to which this latter stretches to the breaking point [11].

c. Compressive Testing

Compression test shows how the material reacts when it is compressed. Compression test is suitable for determining material's behavior or response under crushing loads and for measuring the plastic flow behavior and ductile fracture limits of a material [13].

There are many other types of mechanical testing as: fatigue testing, impact testing, fracture toughness testing… In our study, we're interested about the tensile testing. Its principle is detailed below.

I.4.2. Principle of the tensile testing

Tensile testing is essential for characterizing material's behavior. It is performed by applying increasing tension to the main longitudinal axis L (effective length) of the sample, as shown in Figure I.18. The result of this process is an elongation $\Delta L = L_f - L_i$ [14].

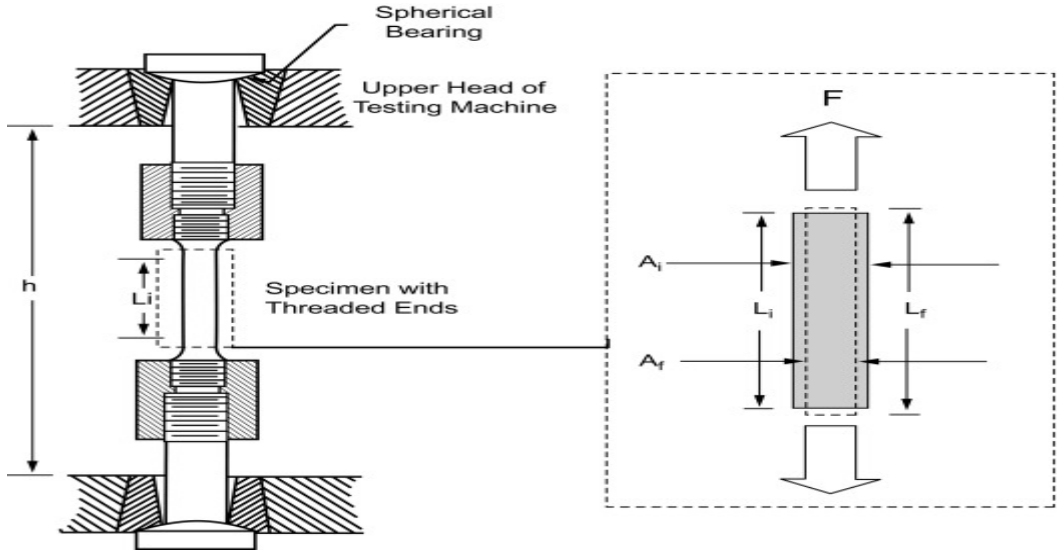

Figure I.18. Principe a typical tensile test [14].

I.4.2.1. Tensile Specimen

The specimen has enlarged ends or shoulders for gripping (Fig.I.19). An important part of the sample is the gage part. The cross-sectional area of the measurement section is reduced relatively to the rest of the sample, so both deformation and failure are concentrated in this area. The gauge length is the area where the measurements were taken and centred in the reduced section. The distance between the gage end and shoulder should be large enough so that the larger ends do not restrict deformation within the gage, and the gage length should be large relative to its diameter [16].

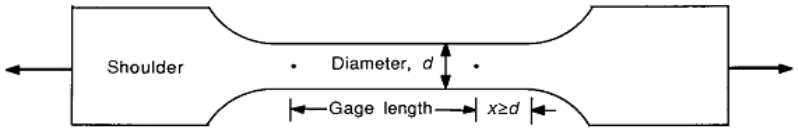

Figure I.19.Typical tensile specimen geometry, showing a reduced gage section and enlarged shoulders [16].

I.4.2.2. Stress-Strain Curve

During the tensile test, the applied tensile force $F$is recorded as a function of the increase in gage length (Fig.I.20-a).

The nominal stress, S, is defined as:

$$S = \frac{F}{A_0} \tag{I.09}$$

$A_0$is the initial cross-sectional area of the gage section.

The nominal strain, e, is defined as:

$$e = \frac{\Delta L}{L_0} \tag{I.10}$$

Where:

L_0: is the initial gage length.

ΔL: is the elongation in gage length i.e. $\Delta L = L - L_0$.$L$is the gage length at time t.

A stress-strain curve, $S = S(e)$, with the same shape as the force-elongation curve can be plotted by using the force-strain data (Fig.I.20-b). The advantage of dealing with stress versus strain rather than load versus elongation is that the stress-strain curve is practically independent of specimen dimensions [15, 16].

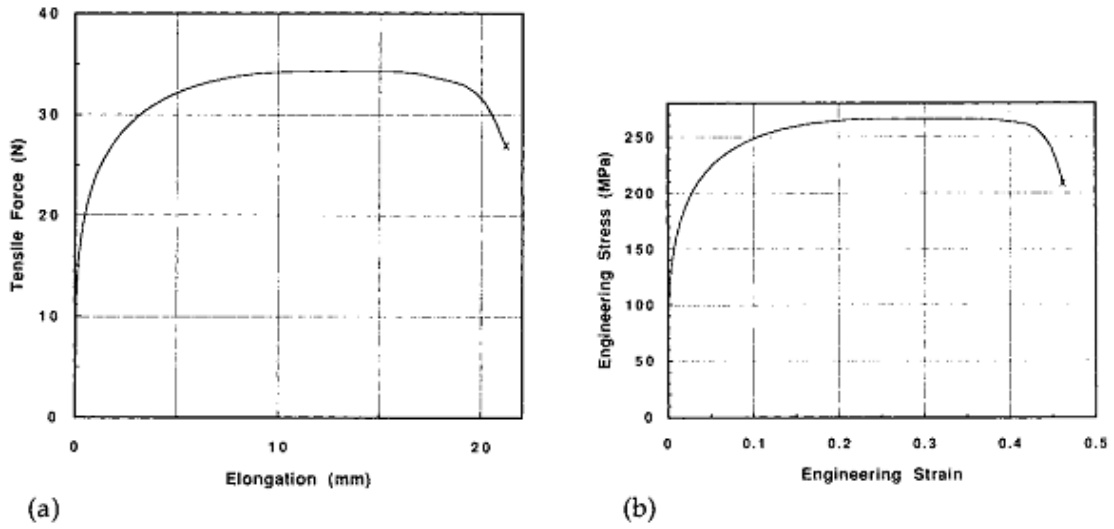

Figure I.20.Example of (a) load-elongation curve from a tensile test and (b) corresponding engineering stress-strain curve.[16].

I.4.2.3. True Stress and Strain

In order to predict a metal's behavior, it is suitable to use the real stress and strain data.

The true stress is defined as:

$$\sigma = \frac{\mathrm{F}}{\mathrm{A}} \tag{I.11}$$

Where A is the instantaneous cross-sectional area at the time that forceF is applied.

The true strain is defined as:

$$\varepsilon = \ln\left(\frac{L}{L_0}\right) = \ln(1 + e) \tag{I.12}$$

Considering an uncompressible material ($L.A = L_0.A_0$), Equations (I.11) and (I.12) become:

$$\sigma = S\,(1 + e) \tag{I.13}$$

$$\varepsilon = \ln(1 + e) \quad \text{(I.14)}$$

Units of measurement: σ in Pascal (Pa), F in Newton (N) and Ain m^2.

At very low strains, the differences between true and engineering stress and strain are very small [16]. Fig.I.21 show the difference between these two curves: $S(e)$and $\sigma(\varepsilon)$.

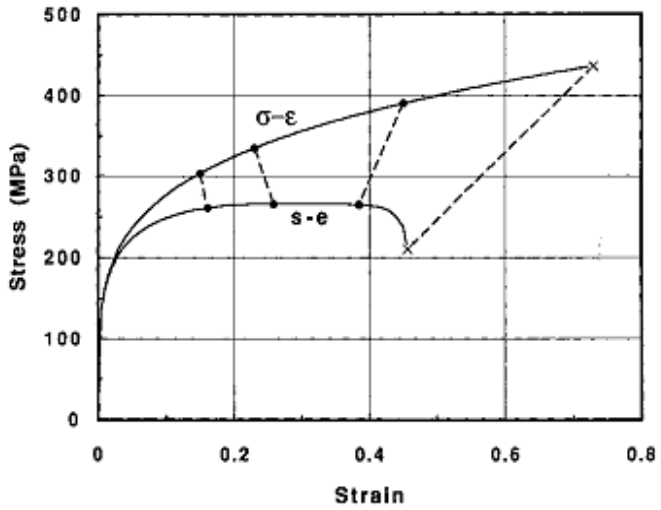

Figure I.21.Comparison of engineering and true stress-strain curves [16].

Figure I.22 shows the evolution of the shape of ductile specimen, the various stages of straining and the different mechanical characteristics which can be determined from a tensile test.

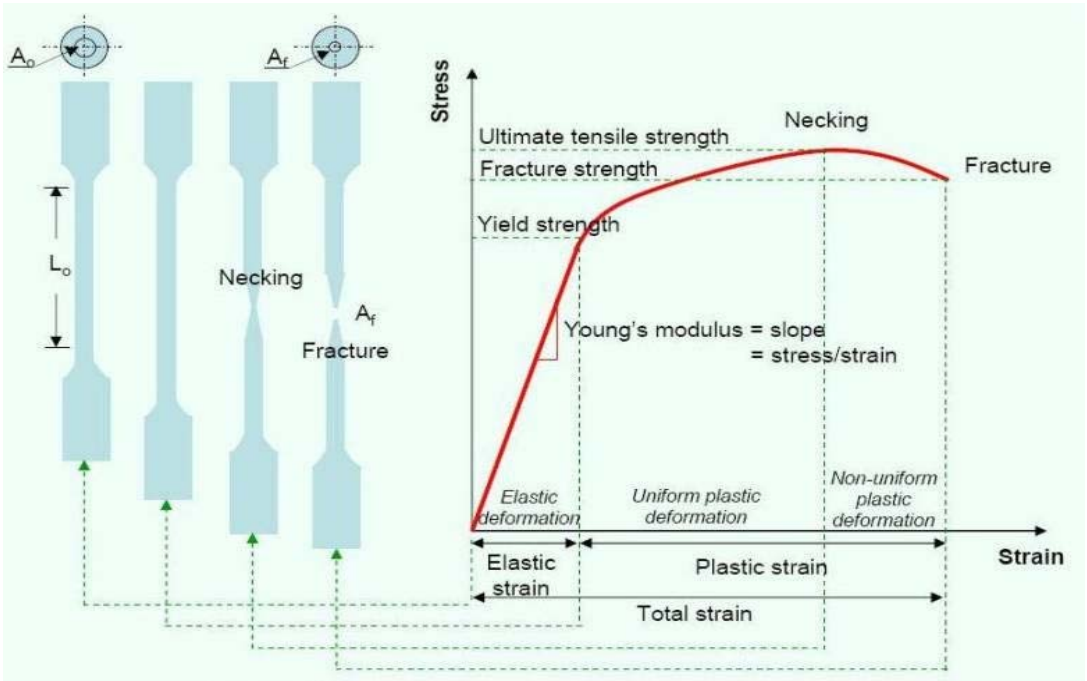

Figure I.22. Stress-strain curve [17].

I.5. Deformation of metallic materials

I.5.1. Elastic and plastic deformation

During a tensile test for example, the specimen length enhances when a sufficient force is applied. At the beginning, the force is proportional to the elongation. The ability of the material to regain its original shape explained as a temporary shape change that automatically reverses after force suppression is called elastic deformation [15, 16].

When the applied stress reaches a certain limit, where it is no longer proportional to the elongation, the material remains deformed even after the withdrawal of the force which caused the change of shape, in this case we are talking about plastic deformation. For most materials, the initial portion of the curve is linear (Fig.I.23). The slope of this linear region is called the elastic modulus or Young's modulus:

$$E = \frac{\sigma}{\varepsilon} \tag{I.15}$$

In reality, the specimen deforms not only in the direction of the traction where there is an elongation but also in the axes where there is shrinking. So in the elastic range, the ratio υof the magnitude of the transverse contraction strain to the axial strain is called Poisson's ratio[16]:

$$\upsilon = -\frac{\varepsilon_r}{\varepsilon} \tag{I.16}$$

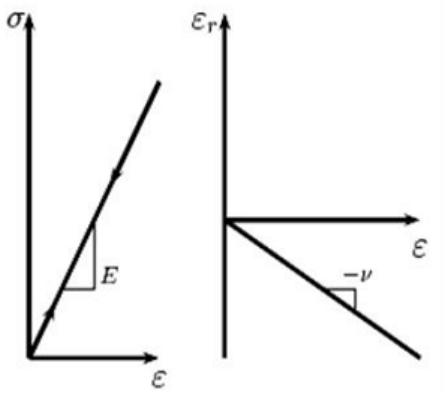

Figure I.23.Simple tensile testing, definition of Young's modulus and Poisson coefficient.

If the stress increases high enough, the stress-strain behavior will no longer be linear and the strain will not completely disappear upon unloading. The remaining strain is called plastic strain. The first plastic strain usually corresponds to the first deviation from linearity (Fig.I.22). Once plastic deformation begins, both elasticity and plasticity contribute to the total strain ε_T. It can benoted $\varepsilon_T = \varepsilon_e + \varepsilon_p$, where ε_p is the plastic contribution and ε_e is the elastic contribution.The onset of plasticity (at stress noted R_e) is usually described by an

offset yield strength (at stress noted $R_{e0.2}$), which can be measured with higher reproducibility. It can be found by constructing a line parallel to the initial linear portion of the stress-strain curve, but offset by ε = 0.002 or 0.2% (Fig.I.24) [16].

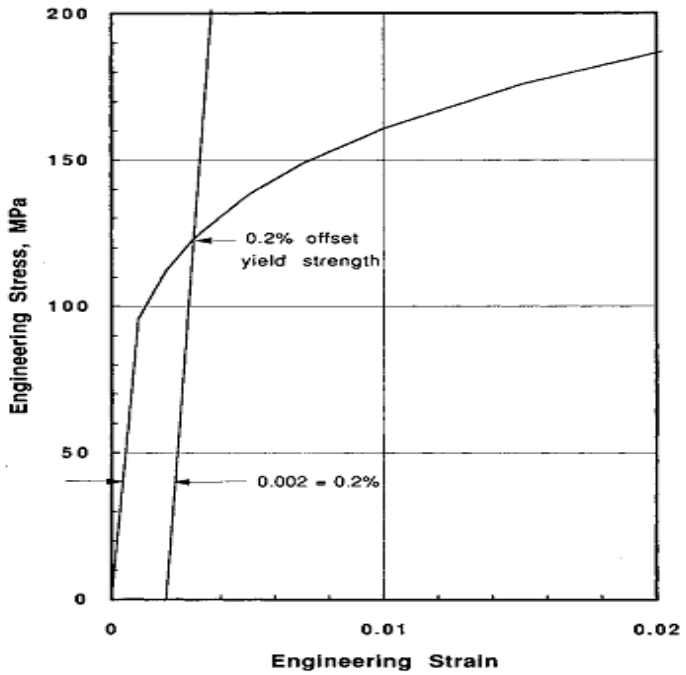

Figure I.24.The low-strain region of the stress-strain curve for a ductile material [16].

Plastic deformation involves the break of a limited number of atomic bands by the movement of dislocations. Recall that the force necessary to break the bands of all the atoms of a crystalline plane at once is very high. However, the movement of dislocations allows atoms of the crystalline planes to slide over each other at much lower stress levels. Since the energy needed to move is lowest along the densest planes of atoms, dislocations have a preferred directions of motion in material. The result is a slip that occurs along parallel planes within grains. These parallel glide planes are grouped together to form glide bands, visible under an optical microscope (Fig. I.13). A slip band appears as a single line under the microscope, but is actually composed of closely spaced parallel glide planes [5,8].

I.5.2. Necking and fracture

On the point of instability, the stress–strain curve is at its maximum (Fig.I.22).At low stress, by making a little neck, the material will work harden and will be able to carry the extra stress it has to stand because of its smaller area; load will therefore be continuous, and the material will be stable. At high stress, the rate of work-hardening ($h = \frac{d\sigma}{d\varepsilon}$)is reduced(Fig.I.22). At a

point of necking (Fig.I.25), the work-hardening rate is only just enough to stand the extra stress with:

$$\frac{d\sigma}{d\varepsilon} = \sigma \tag{I.17}$$

At higher true stress, the work hardening rate decreases and becomes not sufficient to maintain stability. The additional stress in the neck can no longer be accommodated by the work hardening created by the neck, this latter grows faster, until the final fracture happens [18].

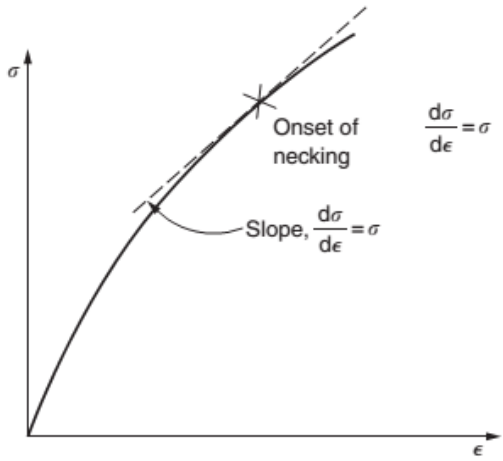

Figure I.25.The condition for necking on the stress-strain true curve[18].

I.6. Conclusion

The bibliographical review about the crystalline structure of metallic materials and their various defects allowed us to understand the different aspects of deformation and the mechanisms associated at microscopic scale. The study of the dislocations which, in turn, are linear defects, allowed us to understand that the plastic deformation is mainly determined by the crystal slide of these dislocations. By the end of this chapter, it can be found that there are a lot of tests that can be used to perceive the mechanical characteristics of the metallic materials during a plastic deformation, the most common of them is the tensile test. It will be used in the 3rd chapter to investigate plastic deformation of an Al-3.2%Mg alloy at room temperature.

Chapter II

Dynamic strain aging and plastic instabilities in metals

Chapter II

Dynamic strain aging and plastic instabilities in metals

II.1. Introduction

At the microscopic scale, due to the presence of obstacles (forest dislocations, precipitates ...), dislocations glide discontinuously in crystalline materials and, consequently, the plastic deformation is always inhomogeneous. At the macroscopic scale, in many cases, plastic flow can be considered homogeneous due to the high density of defects and their random distribution. However, there are many cases where plastic instabilities appear at macroscopic scale. Plastic instability is due to strain localization which is a non-linear phenomenon, leading to the formation of various patterns. The stability analysis methods are early used to study plastic instabilities [19, 20].

Localized deformation causes the initiation of fractures and thus limits ductility and toughness of materials. Strain localization is also of great theoretical interest as it relates to the difficult and unsolved problem of the connection between defects properties and bulk deformation behavior. At the dislocation level, appearance of local strain patterns during plastic deformation is a cooperative phenomenon; it requires the emergence of critical conditions. Therefore, understanding plastic instability needs to identify the microscopic mechanisms of the localization process and incorporate them into constitutive formulations that can be used to predict material responses [20].

For certain metallic materials, such as Al-Mg alloys, under a specific strain rate and temperature conditions, plastic deformation occurs in a very unstable way and appears at the macroscopic scale. It can causes bands formation on the material surface, sometimes visible to the naked eye. Piobert-Lüders and the Portevin-Le Chatelier (PLC) phenomena are the commonly plastic instabilities observed in metallic materials. Strain localizations induce stress drops on the stress-strain curve.

In the present chapter we interested to the Dynamic Strain Aging (DSA) phenomenon in Al-Mg alloys and its consequences at the macroscopic scale, i.e. the appearance of PLC instabilities.

II.2. Heterogeneous mechanical behavior of metallic materials

Before describing the heterogeneity of plastic deformation, it is crucial to remind the usual meaning of homogeneous deformation.

II.2.1. Homogeneous plastic deformation

During a mechanical test, generally, we obtain an identical behavior at each moment at any area of the specimen. Consequently, the strain is assumed homogeneous and the plastic flow is stable. Under these conditions, the curve-strain is regular; the stress increase continuously until the necking of the sample. The macroscopic plastic deformation is then described as homogeneous. This homogeneity property is acceptable only on a sufficiently large scale of observation. An observation on a finer or even microscopic scale reveals that the overall response of a system is in any case obtained from a large number of fully distributed micro-responses randomly [21].

II.2.2. Heterogeneous plastic deformation

In some cases, macroscopic deformation localizes in regions of the specimen and the plastic flow becomes unstable. The stress-strain curves are neither monotonic nor continuous, but exhibit abrupt variations of stress, the typology of which is used to distinguish different forms of heterogeneity. Sometimes, jerky flow is accompanied by acoustic emissions [21].

II.2.3. Types of plastic instabilities

Plastic instabilities manifest themselves in different ways, they can be classified by considering various criterions: their permanent or temporal character, their stationary or propagative character...[22].

In metallic materials, as steels and aluminum alloys, two main types of instabilities are generally observed:

1. Piobert-Lüders instabilities

The Piobert-Lüders (PL)bands are transient heterogeneities; they disappear spontaneously shortly after its first manifestation at yield point and the deformation becomes again macroscopically homogeneous(Fig.II.1)[22].

This type of instabilities is a softening process, it is observed in tensile tests at room temperature in various metallic alloys. The propagation of PL bands is due to the increase in the density of mobile dislocations in the specimen at the onset of plastic flow. In materials with this instability, there are strong interactions between dislocations and obstacles. New dislocations are more likely to be generated in areas of stress concentration. They can be

easily moved, form stacks and activate anchored dislocation sources. Diffusion of mobile dislocations begins at points of stress concentration and propagates in strips from these points under the action of applied stress. Localized regions of plastic deformation, called PL bands, which then propagate as a single front or multiple consecutive fronts(Fig.II.1-b) [36].The deformation becomes homogeneous again when the specimen is filled with bands.

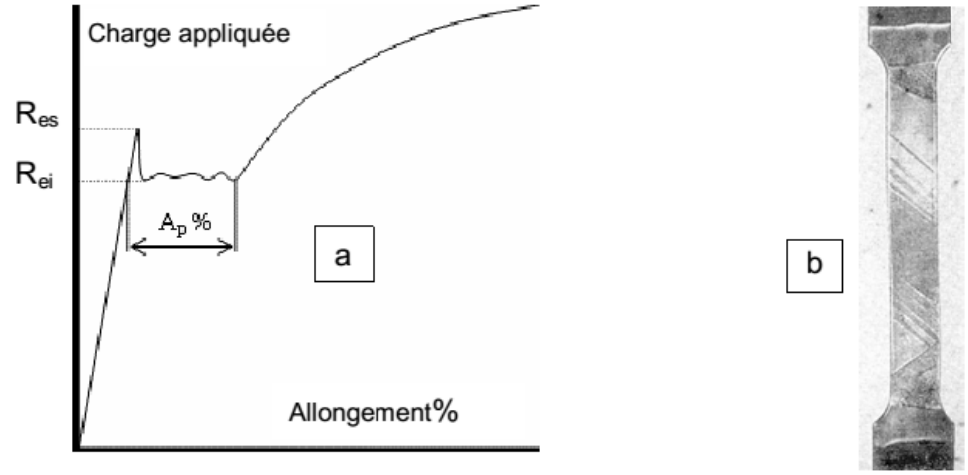

Figure II.1.(a) Schematic representation of a tensile curve with Piobert-Lüders bearing. (b)Strain bands visible on the surface of the specimen [22].

2. Portevin-Le Chatelier instabilities

Bands associated with the Portevin-Le Chatelier (PLC) effect should not be confused with PL bands. The latter constitute a transient phenomenon linked to the existence of a lower limit and an upper limit of elasticity (Fig.II.1-a), whereas the PLC effect can be observed over a wide range of deformation. PL bands cross the surface of the specimen only once while PLC bands reproduce several times. The flow stress remains practically constant during the propagation of the PL bands whereas it increases from one band to the next in the case of the PLC bands. In some materials, as Al-Mg alloys, we can observe the two forms of heterogeneities, the PL bands followed by PLC bands[23, 24].

In the following, we will study PLC instabilities. They originate from the dynamic strain aging mechanism and manifest through various experimental aspects depending on the deformation conditions.

II.3. The Portevin-Le Chatelier effect

II.3.1.Physical origin of the PLC effect: dynamic strain aging of mobile dislocations

The PLC effect was observed as discontinuous plastic flow in several materials, mostly in metallic materials. This phenomenon has attracted the attention of many researchers, and several models based on different approaches have been developed to elucidate the mechanisms responsible for this instability. To date, despite extensive experimental work and all models proposed, there is no clear consensus for a coherent description of the experimental results. Under normal conditions of thermally activated motion, for a given strain condition, the flow stress of mobile dislocations increases with increasing applied strain rate and/or decreasing temperature. Typically, this mechanical behavior is transformed at the macroscopic level by the stabilization of the flow stress leading to a homogeneous macroscopic plastic deformation. For a given strainε, the definition of the sensitivity *S* of the flow stress $\sigma$to the strain rate $\dot{\varepsilon}_a$is given by the expression [22,29, 30]:

$$S(\dot{\varepsilon}_a) = \left(\frac{\partial \sigma}{\partial \ln \dot{\varepsilon}_a}\right)_{\varepsilon} \quad \text{(II.1)}$$

According to this equation, $S(\dot{\varepsilon}_a)$ becomes positive and gives rise to a homogeneous macroscopic plastic deformation when the stress σ increases monotonously with strain rate $\dot{\varepsilon}_a$. However, under certain deformation conditions of metallic materials, solute atoms diffuse to mobile dislocations increasing their flow stress during their temporary arrests at forest obstacles (immobile dislocations, precipitates, etc.). This mechanism is called Dynamic Strain Aging (DSA) of dislocations. The additional stress due to dynamic aging, σ_{DSA}, is an increasing function of waiting time t_w of mobile dislocations at forest obstacles. σ_{DSA} is a decay function of the imposed strain rate $\dot{\varepsilon}_a$ since t_w is inversely proportional to $\dot{\varepsilon}_a$. As a result, in the presence of dynamic aging, the total applied stress σ_{tot} is the superposition of the thermal activation component σ_{activ} and the dynamic aging component σ_{DSA} (Fig.II.2):

$$\sigma_{tot} = \sigma_{activ} + \sigma_{DSA} \quad \text{(II.2)}$$

DSA leads to a reduction in the sensitivity of flow stress to strain rate, which can become negative over a limited range of temperature, strain and strain rate. In this range, plastic flow becomes unstable and strain localizations occurs in narrow bands in the material, associated with stress drops on the stress-strain curve, a discontinuous state also known as jerky flow [17, 31,32].

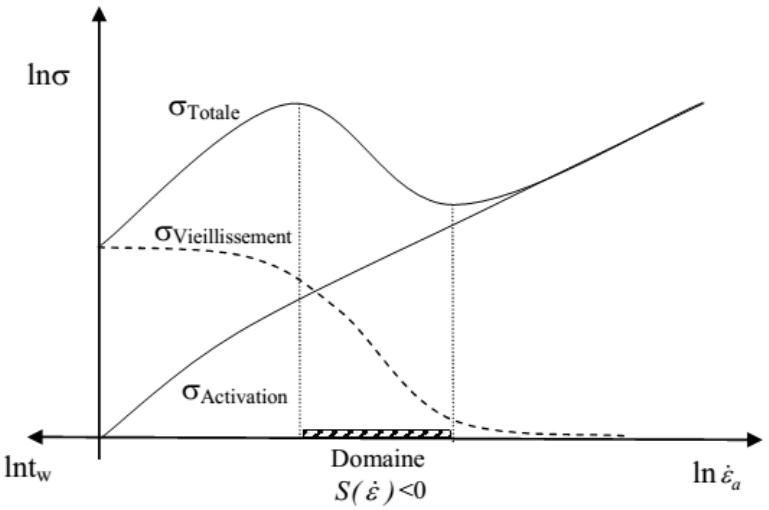

FigureII.2. The Total applied stress is the result of an activation component and an aging component. The hatched area, forbidden to dislocations, represents the domain of appearance of the PLC effect [33].

A negative strain rate sensitivity of flow stress which is a prerequisite for instability of this type occurs in a limited range of temperatures and strain rates, this negative sensitivity can also be seen by varying the applied strain rate during a same tensile test. At the microscopic scale, the effect stems from a dynamic interaction between mobile dislocations and diffusing solute atoms during their temporarily arrests at localized obstacles. Accordingly, the glide resistance decreases with increasing strain rate, i.e. with decreasing waiting time at obstacles [19, 24].

In tensile tests, at constant applied strain rate, PLC instability is characterized by the appearance of typical stress drops on the mechanical response curve (Fig.II.3). Associated bands appear locally and propagate in form of bands on the specimen surface during loading, leading to strong stress variations [21].Outside the range of instability, the deformation curves are smooth and an increase in the strain rate leads to an increase in stress [21].

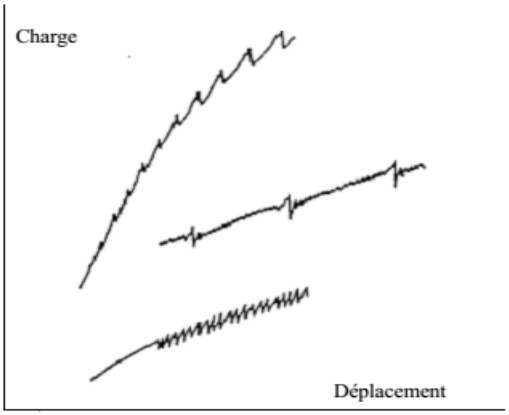

FigureII.3. Examples of Portevin-Le Chatelier plastic flow instabilities at different applied strain rates [21].

PLC bands appear after more or less work hardening of the deformed sample. They are then propagating, for example by repeatedly filling the working area of the deformed specimen. The specimen hardening is caused by the passage of series of bands, requiring an increase in the applied load to reach the yield stress and start the next series of bands [27].

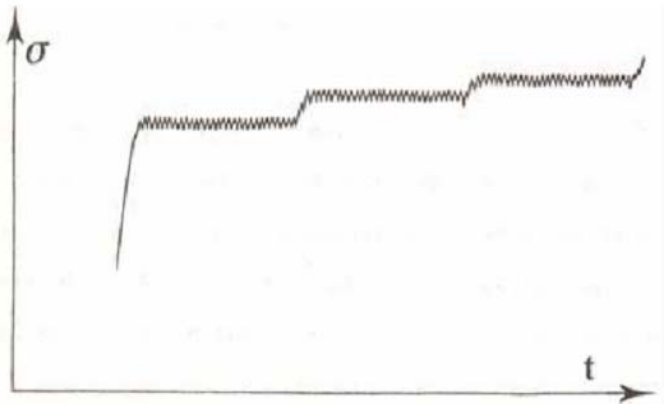

FigureII.4. Instabilities with reload periods [27].

In tension mode at constant loading rate (soft testing machine), the appearance of PLC instabilities differs from that observed at imposed strain rate (hard testing machine). At constant loading rate $\dot{\sigma}$, once a band is formed, it immediately begins to move and passes through a part or the entire specimen at a very high velocity. The passage of each band causes a work hardening in the specimen, the next band requires a higher stress and thus the obtained tensile curve has a pronounced stepped appearance (Fig.II.5)[27].

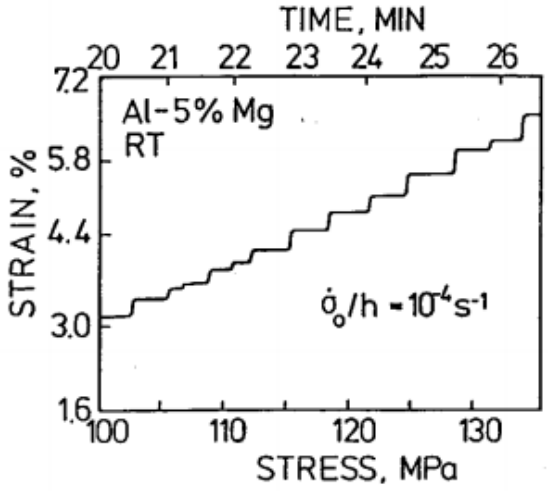

FigureII.5. Strain jumps in Al-5%Mg deformed at room temperature at constant loading rate [28].

II.3.2. Experimental aspects of PLC instabilities

II.3.2.1. Spatial aspect

Due to DSA mechanism, strain localizes in narrow zones (bands) inclined with respect to the tensile axis. During straining, the specimen is covered with bands for several times as it expands under an increasing stress. Depending on the applied strain rate, at a given temperature, the PLC bands propagate more or less correlated or appear randomly on the surface of the specimen. These bands can be clearly observed on the specimen surface (Fig.II.6) with the naked eye and sometimes under appropriate lighting conditions [23].

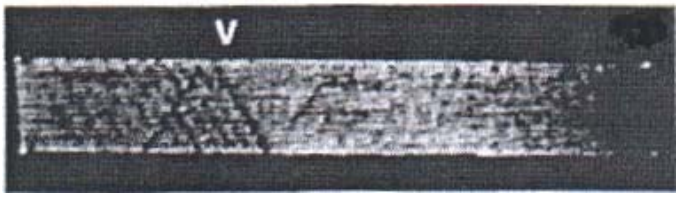

FigureII.6. Traces of PLC bands on the sample surface: actual image after passing several bands [27].

II.3.2.2.Temporal aspect

Strain localizations due to the PLC effect induce typical stress drops more or less abrupt on the deformation curve (Fig.II.3). Each drop corresponds to an instability of the plastic flow of the material. The stress drop magnitude (Fig.II.7), $\Delta\sigma$, recorded on the stress-strain curve gives an indication on the intensity of PLC instability. It is considered as an indicator of the degree of heterogeneity of plastic deformation [21, 25].

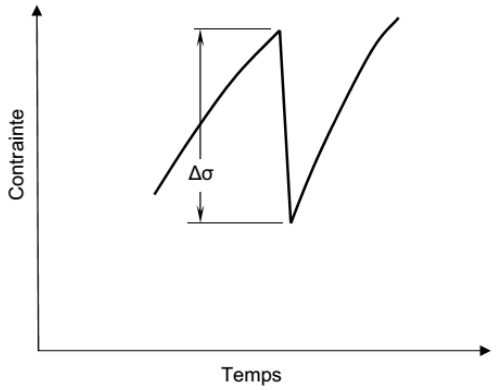

FigureII.7. Schematic representation of an oscillation on the deformation curve with definition of the magnitude of the stress drop [21].

II.3.2.3.Types of PLC instabilities

PLC pattern observed on the specimen surface and on the stress-strain curve depends on the microstructure of the deformed material and the imposed external conditions of temperature and strain rate. The recorded curve shows a more or less periodic succession of discontinuities characterizing the types of bands. There are three types of PLC instabilities:

Type A instabilities

Type A instabilities are observed at low temperatures or/and high strain rates (Fig.II.8-a). This type of instability is associated to the propagation of the plastic strain band front on the sample. Once formed, each band propagates continuously over part or the entire specimen (Fig.II.8-b) [27, 34]**.**

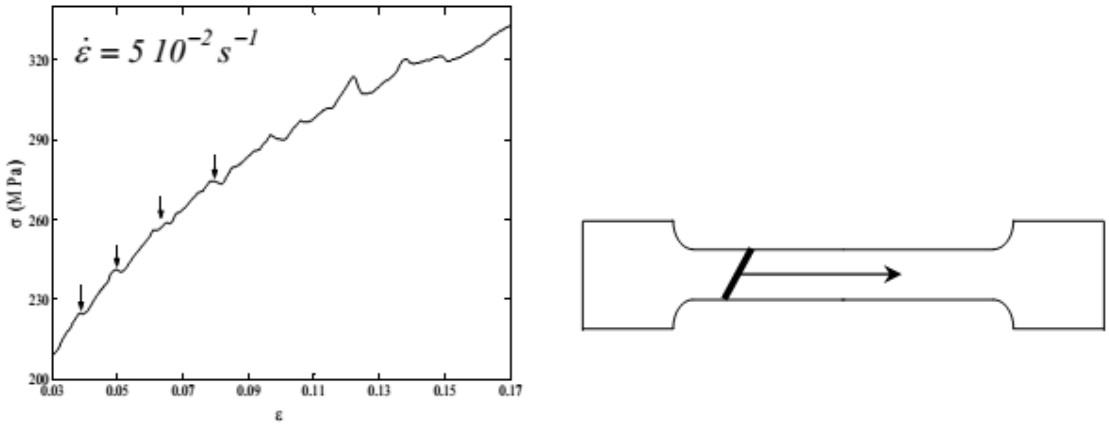

(a) (b)

FigureII.8. (a) Stress-strain curve showing type A instabilities in Al-3.2%Mg alloy [17]. (b) Kinematic aspect of type A bands[21].

Type B instabilities

Type B instabilities appear for intermediate temperatures and strain rates. They move discontinuously (hopping bands) and produce regular stress drops on deformation curves(Fig.II.9). From a band to another, an additional reloading is required each time to activate a new band [23].

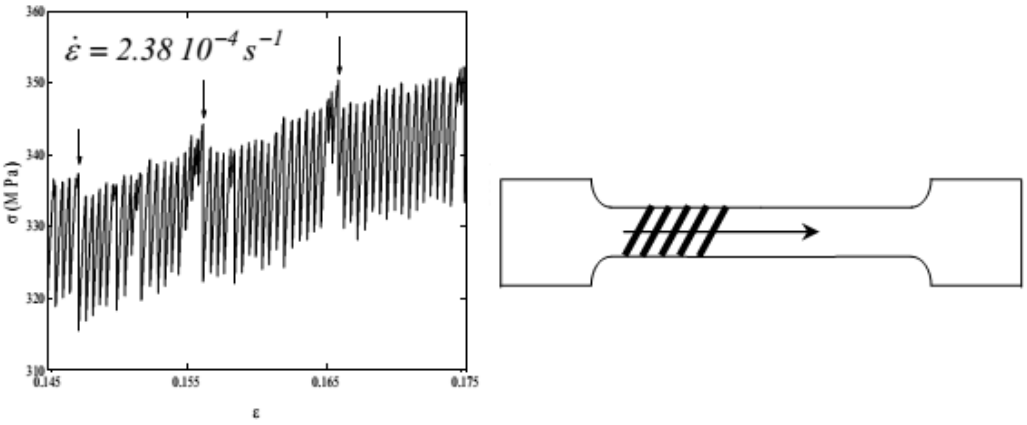

(a) (b)

FigureII.9. (a) Stress-strain curve showing type B instabilities in Al-3.2%Mg alloy [17]. (b) Kinematic aspect of type B bands[21].

Type C instabilities

Type C instabilities appear at very low strain rates and/or high temperatures. Associated stress drops on the stress-strain curve are large (Fig.II.10-a), producing at each instability an intense

localization. The work hardening is very low. The associated deformation bands appear randomly on the surface of the deformed material and are static (not propagative) (Fig.II.10-b) [23].

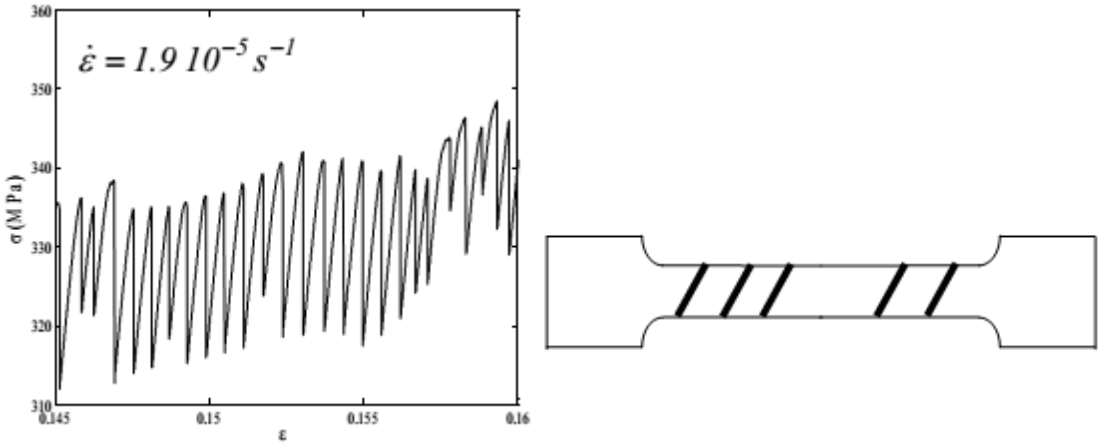

(a) (b)

FigureII.10. (a) Stress-strain curve showing type A instabilities in Al-3.2%Mg alloy [35]. (b) Kinematic aspect of type C bands, with random appearance [21].

II.3.2.4.Critical plastic strain for the onset of instabilities

A jerky flow recorded as serrations on the stress-strain curves (hard testing machine) or as strain bursts under loading (soft testing machine) with constant stress rate, often sets in after a finite incubation strain ε_c [19]. For a given temperature to the appearance of PLC instabilities and from a certain critical deformation rate $\dot{\varepsilon}_1$, the plastic flow stress continuously decreases from $\dot{\sigma}_1$ to $\dot{\sigma}_2$ while the rate of deformation changes from $\dot{\varepsilon}_1$ to $\dot{\varepsilon}_2$ (Fig.II.11). Macroscopic sensitivity to strain rate is negative [21, 25].

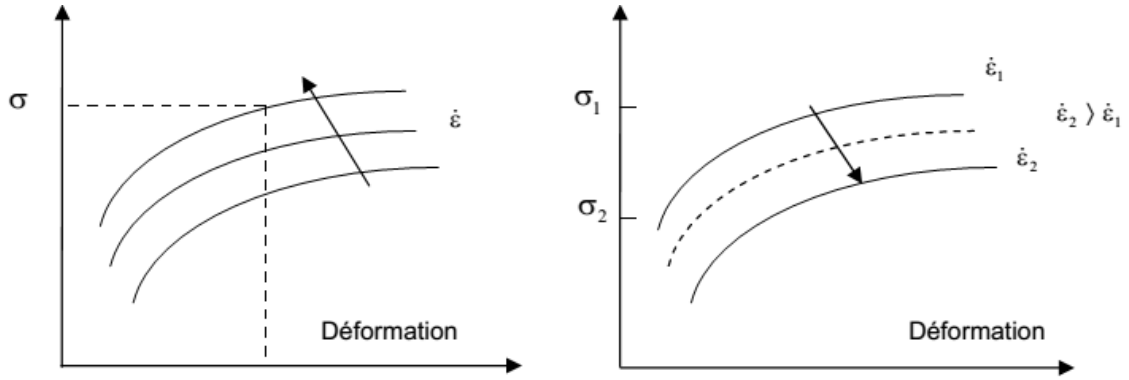

(a) (b)

FigureII.11. Schematic representation of the evolution of flow stress as a function of the strain rate. The arrow indicates the direction of increase of the imposed strain rate. For a given strain ε, the sensitivity to the strain rate is: (a) positive outside critical values,(b) negative inside [21].

The critical plastic strain for the onset of instabilities ε_c marks the transition “stable plastic flow - unstable plastic flow”. This limit is affected by several factors, such as temperature, strain rate and the microstructure of the deformed material. At high strain rates and/or low temperatures, ε_c increases with the increase in strain rate (or a decrease in temperature). This is called "normal behavior" of ε_c. At low strain rates and/or high temperatures, ε_c decreases with the increase in strain rate(or a decrease in temperature). This is called "inverse behavior" of ε_c. An example of these behaviors, at a fixed temperature, is shown in Fig.II.12 [26].

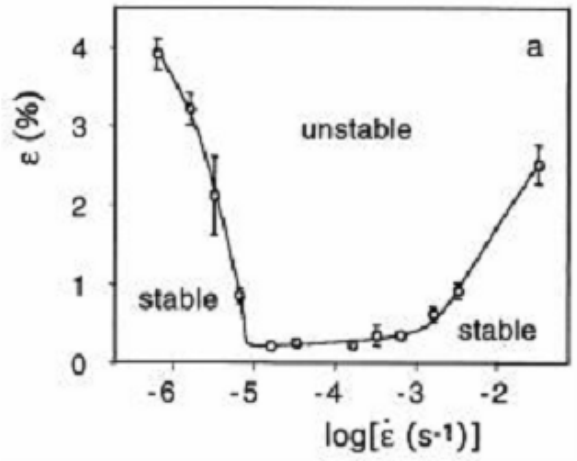

FigureII.12. Evolution of the critical strain for the appearance of PLC instabilities in Al-2.6%Mg at room temperature [26].

II.4. Conclusion

The present chapter allowed us to understand the different experimental aspects of the PLC effect. Depending on the imposed deformation conditions, it manifests itself in various ways. This phenomenon is of particular interest of many researchers in the fields of materials sciences and metallurgy. Despite the development of experimental devices and computer tools, a satisfactory description of these various aspects has not yet been proposed. To date, no theoretical model has allowed reproducing different experimental aspects of the PLC effect. Among the various theoretical approaches, the theoretical approach based on dynamic strain aging mechanism explains several experimental aspect of the PLC effect. DSA is currently considered to be responsible for the negative strain rate sensitivity of the stress flow. However, there is a difficult to make the transition from microscopic to macroscopic scale. In particular, describing the formation and displacement of strain bands, the inverse behavior of critical strain.

In the next chapter, using tensile tests, we investigate experimental aspects of jerky flow in an Al-3.2%Mg alloy at room temperature.

Chapter III

Analysis of stress drops associated to jerky flow in the Al-3.2%Mg alloy

Chapter III
Analysis of stress drops associated to jerky flow in the Al-3.2%Mg alloy

III.1. Introduction

Aluminum alloys have a wide range of applications due to their interesting properties. They are used in many and different applications, particularly in corrosive environments. A typical example of these alloys is the 5xxx series (Al-Mg alloys), which have excellent corrosion resistance and very good mechanical properties to withstand the harshest conditions such as marine environments.

During plastic deformation of Al-Mg alloys, the magnesium can diffuse and interact with mobile dislocations. Under certain conditions, this dynamic interaction leads to strain localizations of Portevin-Le Chatelier (PLC) type. In the following, we study jerky flow and mechanical characteristics of the Al-3.2%Mg alloy during tensile tests at room temperature. We analyze the effect of the strain and the imposed strain rate on the mechanical behavior and the different patterns associated to instabilities.

Under the imposed deformation conditions, we will also be interested in the stress drops distribution which can indicate the degree of spatial correlation between plastic events occurring during plastic deformation.

III.2. Studied material and experimental conditions

III.2.1. Aluminum and its alloys

Aluminum is a lightweight, ductile and malleable metallic material. The major advantages of using aluminum are tied directly to its' remarkable properties. It has strength to weight ratio. It is a good electrical and thermal conductor. When in contact with the

atmosphere, it is covered by a very compact oxide layer (Al_2O_3), which makes it very resistant to corrosion, the quality-price ratio of aluminum and its alloys makes it indispensable for applications in various fields (automotive, aviation, transportation, construction and building etc.). An aluminum alloy is a composition consisting mainly of aluminum to which other elements have been added. The alloy is made by mixing together the elements when aluminum is molten (liquid), which cools to form a homogeneous solid solution. The other elements may make up as much as 15 % of the alloy by mass.

In general, there are two broad types of aluminum alloys: wrought alloys and casting alloys. Both of these groups are subdivided into heat-treatable and non-heat-treatable types. Around 85% of aluminum is used in wrought alloys. Cast alloys are relatively inexpensive to produce because of their low melting point, but they tend to have lower tensile strengths than their wrought counterparts.

Casting alloys: They are used in foundries (relatively low melting temperature ~660°C) to produce parts by pouring liquid metal.

Wrought alloys: They are cast in foundries in the form of slabs or billets and then converted into semi-finished products (sheets, profiles, etc.) by rolling, spinning....

Al-Mg alloys are work hardenable, have moderately high strength, and very high toughness even at low temperatures near absolute zero (-270°C). They can be easily welded using a variety of techniques, even with thicknesses up to 20 cm. As a result, 5xxx alloys are widely used in civil engineering, highway structures (including bridges, storage tanks, …), cryogenic storage tanks, and systems and marine applications with temperatures as low as -270°C (near absolute zero). Magnesium has significant solubility in aluminum and imparts significant solid solution strengthening which also contributes to improved work hardening properties [22,34]. 5xxx series alloys (with <~6% Mg) do not age. While Mg_2Al_3 may precipitate in systems with more than 3% Mg, this phase is not a strengthening precipitate and actually weakens the alloy (by depleting dissolved Mg). Al-Mg alloys derive their strength mainly from solution strengthening and work hardening during deformation.

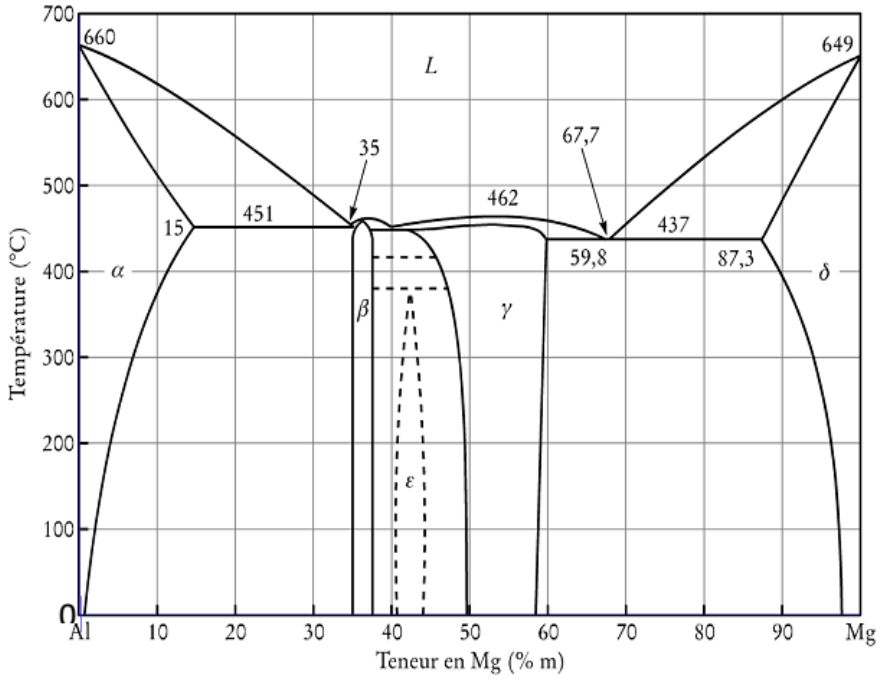

FigureIII.1. Phase Equilibrium Diagram of Al-Mg Alloys [38].

III.2.2. Studied material and experimental conditions

The material used in this study is an aluminum 5754 cold-rolled sheet, referred to below as Al-3.2% Mg alloy. Its chemical composition is given in Table III.1.

Alloy	Mg	Mn	Si	Fe	Cu	Zn	Ti	Cr
Al-3.2%Mg	3.218	0.475	0.165	0.296	0.055	0.043	0.035	0.094

Table III.1. Chemical composition of the Al-3.2%Mg alloy (in wt.%)[36].

Tensile polycrystalline flat specimens were machined in the rolling direction and deformed in tension at room temperature using an Instron 5569 hard testing machine (with a 50 KN load cell). In the studied alloy, at room temperature, PLC instabilities are observed in the strain rates range 10^{-6}-10^{-1} s^{-1}[35].

A total of 10 mechanical tensile tests were conducted at room temperature on the Al-3.2%Mg alloy. Table III.2 summarizes the experimental conditions under which these tests were carried out. Half of the tests were carried out on samples in the reception state (polycrystalline sheet, without additional treatment). The other half of the tests were carried out on samples whose surface has undergone fine polishing, to study the state of the surface on PLC instabilities.

Tensile tests were carried out using five strain rates: 2.38 10^{-4} s^{-1}, 1.19 10^{-3} s^{-1}, 5 10^{-3} s^{-1}, 10^{-2} s^{-1} and 5 10^{-2} s^{-1}. Each strain rate is used to deform a specimen with polishing and another

without polishing. Specimens dimensions are indicated in table II.2. There is a slight reduction in dimensions after polishing.

Test results (displacement, time and load) are provided in digital format. The analysis of the data and the determination of the mechanical characteristics in traction were carried out using the MATLAB software.

Tensile test name	Strain rate (s^{-1})	Imposed velocity (mm/mn)	Specimen dimensions (mm^3)	
			without polishing	with polishing
PLC46	$2.38\ 10^{-4}$	0.6	6.5*1.94*42	
PLC47	$2.38\ 10^{-4}$	0.6		6.26*1.90*42
PLC48	$5\ 10^{-2}$	126	6.5*1.94*42	
PLC49	$5\ 10^{-2}$	126		6.26*1.90*42
PLC50	$1.19\ 10^{-3}$	3	6.5*1.94*42	
PLC51	$1.19\ 10^{-3}$	3		6.26*1.90*42
PLC55	10^{-2}	25.2	5.65*1.94*42	
PLC56	10^{-2}	25.2		5.65*1.92*42
PLC57	$5\ 10^{-3}$	12.6	5.7*1.94*42	
PLC58	$5\ 10^{-3}$	12.6		5.62*1.90*42

Table III.2. Mechanical tensile tests performed at different applied strain rates and at room temperature on the Al-3.2%Mg alloy.

III.3. Deformation curves analysis

For the imposed strain rates $2.38\ 10^{-4}\ s^{-1}$, $1.19\ 10^{-3}\ s^{-1}$, $5\ 10^{-3}\ s^{-1}$, $10^{-2}\ s^{-1}$ and $5\ 10^{-2}\ s^{-1}$, the plastic flow is unstable in the Al-3.2%Mg alloy at room temperature. For an imposed driving velocity, the uniform plastic flow becomes unstable beyond a certain critical plastic strain and remains such until failure by necking. PLC instability pattern depends on the imposed strain rate, the strain level and the surface state (with or without polishing).

In order to take account for variations in the dimensions of the specimen during deformation, the tensile data were corrected. The true values (corrected) of stress and strain are obtained using the equations (I.13) and (I.14). We did the same for all the other tests.FigureIII.2 shows the conventional and corrected (true) curves of the Al-3.2%Mg alloy at room temperature and at an imposed driving velocity of 126 mm/min.

Fig. III.2. shows that the material deforms initially elastically to a yield stress (elastic range), then it deforms plastically until the necking point occurs for maximum elongation (plastic range). Beyond this limit, the material deforms with a decreasing stress until it completely breaks (fracture range) [37].

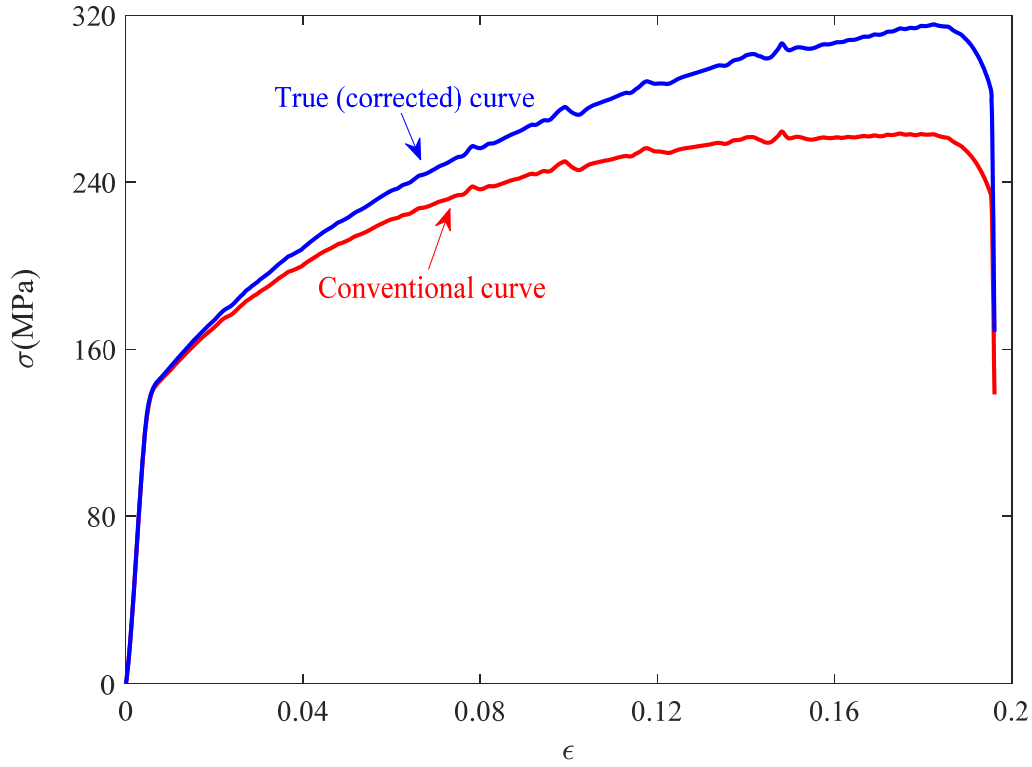

Figure III.2. Tensile curves, conventional and true (corrected), of the Al-3.2%Mg alloy at room temperature and at imposed driving velocity of 126 mm/min.

In order to study the effect of surface polishing jerky flow, we made two tests with each strain rate and with different types of surface (polished or not). FigureIII.3 shows the tensile test curves for the specimen with polishing surface and the other without a polishing at imposed strain rate of 5 $10^{-3}s^{-1}$. The Insert in Fig.III.3 shows clearly that additional nodulations between two successive stress drops associated to bands formations are less pronounced in the curve corresponding to the polished specimen. Surface obstacles reductions by polishing facilitate type A band propagation.

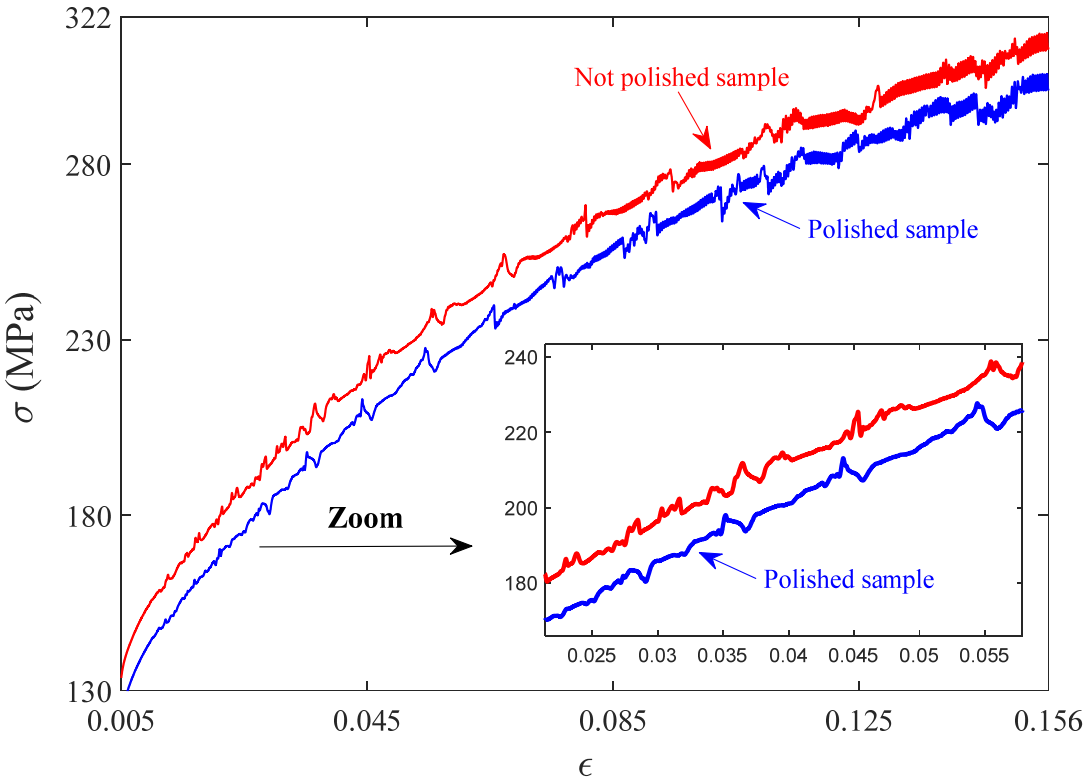

FigureIII.3. Tensile curves of polished and unpolished samples of Al-3.2%Mg alloy at room temperature and at imposed tensile velocity of 12.6 mm/min. For a better view, the curve of the polished sample is shifted downwards by 10 MPa.

III.4. Mechanical and jerky flow characteristics

Mechanical characteristics and jerky flow parameters are determined from deformation curves at room temperature in the instability strain rate range. Figure III.4 shows an example of tensile curve of the Al-3.2Mg alloy, deformed with a strain rate of 2.38 10^{-4} s^{-1}, and the various parameters which can be determined from this curve. Table III.3 shows the obtained results from the analysis of all the tensile tests carried out.

In what follows, we have analyzed the effect of the imposed strain rate $\dot{\varepsilon}_a$on the following mechanical characteristics:

- Young's modulus (E), which corresponds to the slope of the linear part of the stress-strain curve for a material.
- The Yield Strength ($R_e$and $R_{e0.2}$), which corresponds to the yield point at which the material begins to deform plastically.
- The Ultimate Tensile Strength (R_m), corresponding to the onset of necking (Considère criterion).

From the deformation curves, E, $R_{e0.2}$and R_m are determined for various applied strain rates.

The elastic deformation range represents the beginning of the deformation; we can notice it from the proportionality between the deformation and the stress. The proportionality factor corresponds to the Young's modulus (E). In this field, when the force applied is stopped, the material returns to its original form without any residual deformation. For the plastic deformation range which comes just after the elastic deformation, beyond the yield stress R_e (yield stress $R_{e0.2}$). In this phase, the material continues to deform with increasing stress until a certain maximum value R_m. The necking and fracture or the limit-to-break range is from the maximum of the conventional curve that the stress is concentrated in an area of the specimen until its shrinkage leads to the fracture of the specimen [37].

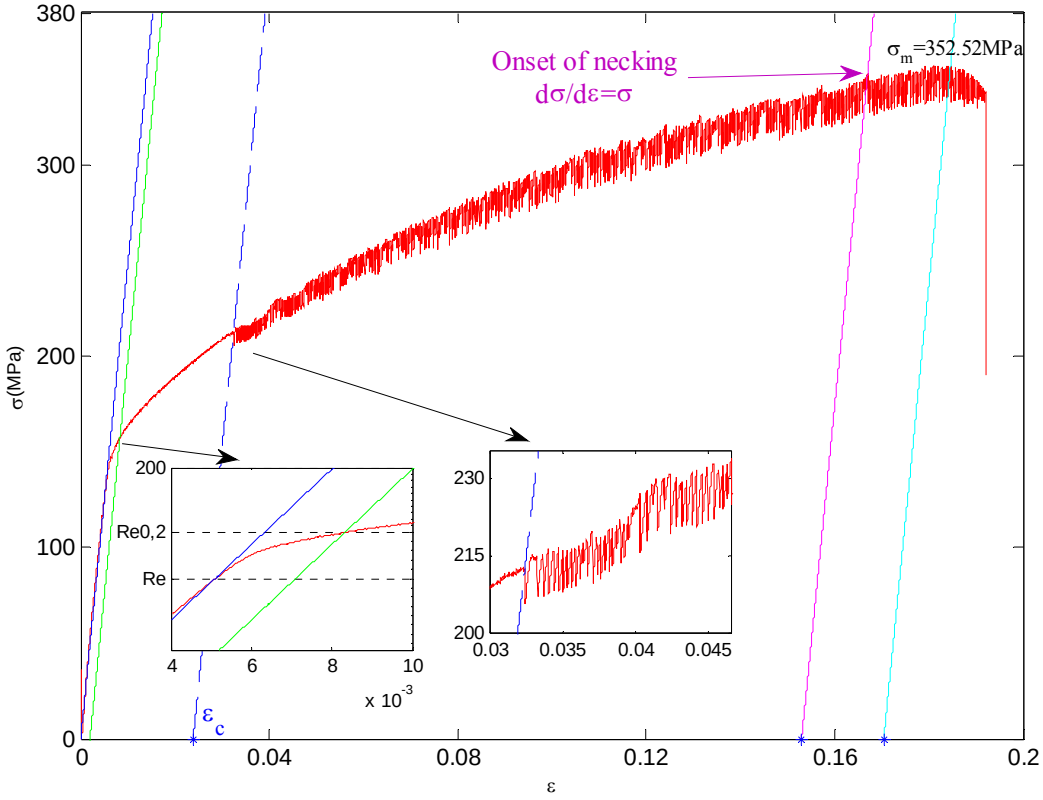

Figure III.4. Tensile curve of the Al-3.2Mg alloy deformed with a rate of deformation of 2.38 $10^{-4}s^{-1}$ showing the different mechanical characteristics.

N°	Test name	$\dot{\varepsilon}(s^{-1})$	Mechanical characteristics					Jerky flow parameters		
			E (GPa)	R_e (MPa)	$R_{e0.2}$ (MPa)	R_m (MPa)	σ_m (MPa)	ε_c	ε_r	ε_{r2}
01	PLC46	2.38 10^{-4}	29.867	127	157.6	294.497	352.520	0.0239	0.1530	0.1704
02	PLC47	2.38 10^{-4}	31.416	123.5	150.7	289.820	345.206	0.0199	0.1587	0.1655
03	PLC50	0.0012	31.120	106.2	152.4	287.937	346.1311	0.0052	0.1715	0.1782
04	PLC51	0.0012	31.003	106.1	144.9	276.120	329.808	0.0064	0.1586	0.1690
05	PLC57	0.005	31.133	104.4	144.5	273.071	327.775	0.0062	0.1674	0.1746
06	PLC58	0.005	31.141	113.3	143	272.841	322.391	0.0061	0.1555	0.1589
07	PLC55	0.01	32.375	104.4	144	271.871	322.814	0.0085	0.1567	0.1634
08	PLC56	0.01	31.184	102	140.1	267.916	320.592	0.0076	0.1690	0.1693
09	PLC48	0.05	31.787	112.9	146	266.642	316.825	0.0156	0.1622	0.1627
10	PLC49	0.05	32.277	95.7	142.7	264.463	315.745	0.0158	0.1386	0.1727

TableIII.3. The mechanical characteristics obtained during the tensile tests.

Fig.III.5 shows the strain rate dependence of the mechanical characteristics. According to the figures, it can be concluded that the polishing performed does not affect significantly the mechanical characteristics, the evolution of the young's modulus is proportional to the strain rate$\dot{\varepsilon}_a$, unlike R_e and R_m decrease with the increase of strain rate $\dot{\varepsilon}_a$.

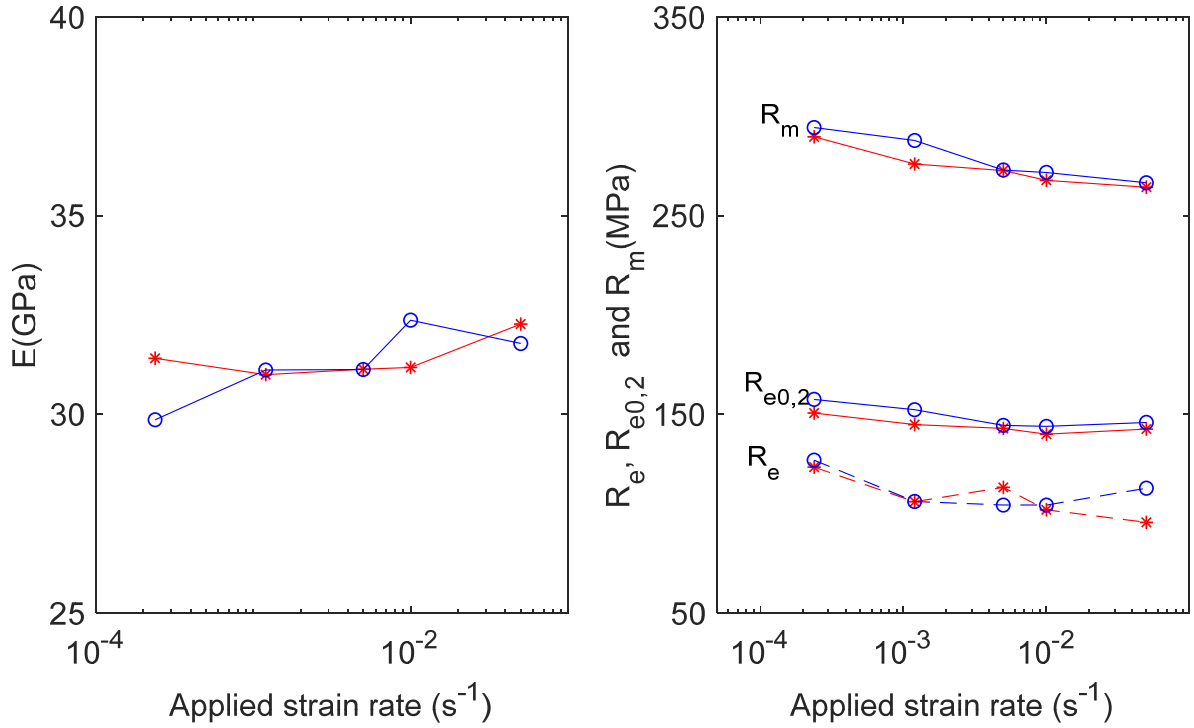

Figure III.5. Applied strain rate dependence of the Young's modulus (E), the Yield Strength($R_e$and $R_{e0.2}$) and the Ultimate tensile strength (R_m) in the Al-3.2%Mg alloy at room temperature.("*" Polished samples; "o": As-received Samples).

Jerky flow parameters are also determined from the stress-strain curves. At the beginning of the plastic deformation the curve is smooth (stable). This indicates the homogeneous character of the plastic flow. But, beyond a certain plastic critical strainε_c, the curve becomes unstable; this shows that the deformation of the material becomes non-homogeneous. The material deforms differently from a zone to another until a characteristic plastic strain at failure, ε_r. The obtained stress-strain curves show that the instability pattern depends on the strain and on the imposed strain rate. Patterns are characterized by the magnitude of stress drops, $\Delta\sigma$, and the reloading time between two successive stress drops, Δt. The strain and strain rate dependencies of jerky flow parameters will be roughly analyzed below.

III.5.Jerky flow characteristics analysis

III.5.1.Critical strain for the onset of instabilities and plastic strain at failure

Fig.III.6 shows the strain rate dependence of the critical plastic strain for the onset of PLC instabilities, ε_c, and of the plastic strain at failure, ε_r,in the Al-3.2%Mg alloy at room temperature. These results show that these characteristics depend on the applied strain rate$\dot{\varepsilon}_a$.

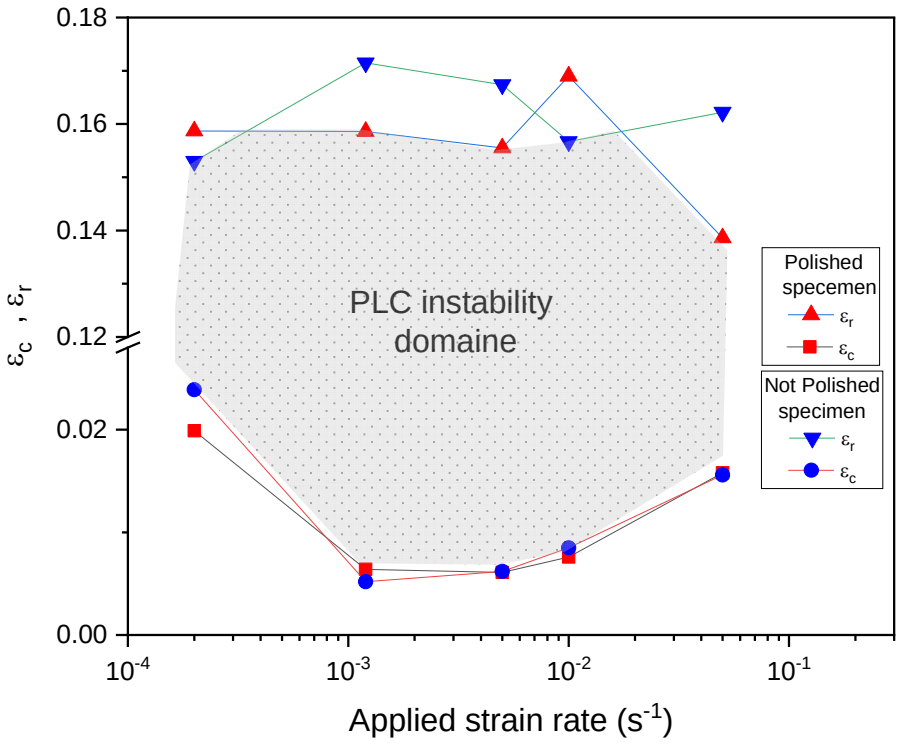

Figure III.6. Applied strain rate dependence of the critical plastic strain ε_c and the plastic strain at failure ε_r in the Al-3.2%Mg alloy at room temperature for polished sample and as-received (not polished) Sample.

The critical plastic strain$\varepsilon_c$decreases then increases when the applied strain rate $\dot{\varepsilon}_a$ increases. The increasing branch of $\varepsilon_c(\dot{\varepsilon}_a)$ corresponds to the "normal behavior". The decreasing branch corresponds to the "inverse behavior". The normal behavior of ε_c can be explained in accordance with the DSA mechanisms of mobile dislocations [39]. For an applied strain rate $\dot{\varepsilon}_a$, the plastic flow becomes unstable, i.e. the DSA becomes efficient, when the solute (Mg) concentration around the dislocations becomes sufficient to produce an additional stress which can make the SRS negative. This critical condition is achieved by increasing the strain until a value ε_c. With increasing $\dot{\varepsilon}_a$, the waiting time of mobile dislocations t_w decreases and, consequently, the critical condition of instability is only reached after an additional hardening. Thus, the increase of $\dot{\varepsilon}_a$delays the onset of instabilities and, consequently, ε_c increases with increasing $\dot{\varepsilon}_a$. However, for the decreasing branch of ε_c, at low strain rates, there is no consensual explanation in the literature to explain this inverse behavior [39, 41].

In the instability domain, DSA also affects the ductility of the deformed material. It manifests itself by a nonmonotonic strain rate dependence of the strain at failure ε_r (ductility-plateau). In some cases, the negative SRS produces a ductility-hole in the PLC strain rates domain [40].

III.5.2. Magnitude of stress drops and reloading time between successive instabilities

As shown in Fig.III.7, the average magnitude of stress drops, $\Delta\sigma_m$, increases with strain for an imposed strain rate. This increase is followed by a progressive saturation of $\Delta\sigma_m$ which becomes almost constant from at high strains. This behavior is due to the multiplication of dislocations, particularly the forest dislocations (obstacles) which enhance the waiting time t_w of mobile dislocations and, consequently, intensify DSA mechanism.

By comparing the two curves, at strain rates 2.38 10^{-4} s^{-1} and 1.19 10^{-3} s^{-1}, we can see that $\Delta\sigma_m$ is inversely proportional to the applied strain rate. At a given strain, a strain rate increase reduces the waiting time t_w of mobiles dislocations at obstacles and DSA, which leads to a decrease of $\Delta\sigma_m$.

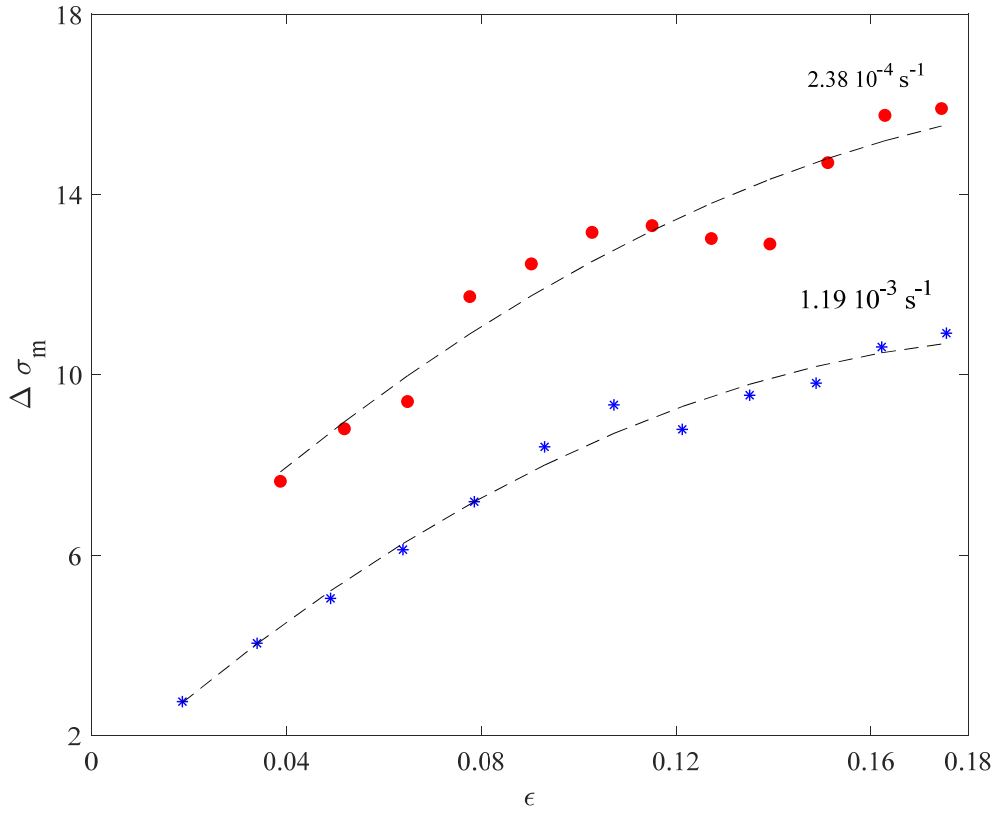

Figure III.7. Strain dependency of the average magnitude of stress drops $\Delta\sigma_m$ at strain rates 2.38 10^{-4} $s^{-1}$and 1.19 10^{-3} s^{-1}in the Al-3.2%Mg alloy.

Figure III.8. shows the variation of the average reloading time between two successive instabilities Δt_m as a function of strain in the Al-3.2% Mg alloy at strain rates 2.38 10^{-4} s^{-1} and 1.19 10^{-3} s^{-1}. It can be seen that at the same strain rate, Δt_m increases during straining. It is related to the strong interaction of mobile dislocations with solute atoms stopping at forest dislocations. By comparing the two curves, we can see that the reloading time between two successive instabilities increases with the decrease of the applied strain rate. It is therefore concluded that, due to DSA, the sensitivity of the reloading time to the strain rate is of the same type as that of the magnitude of the stress drops (negative).

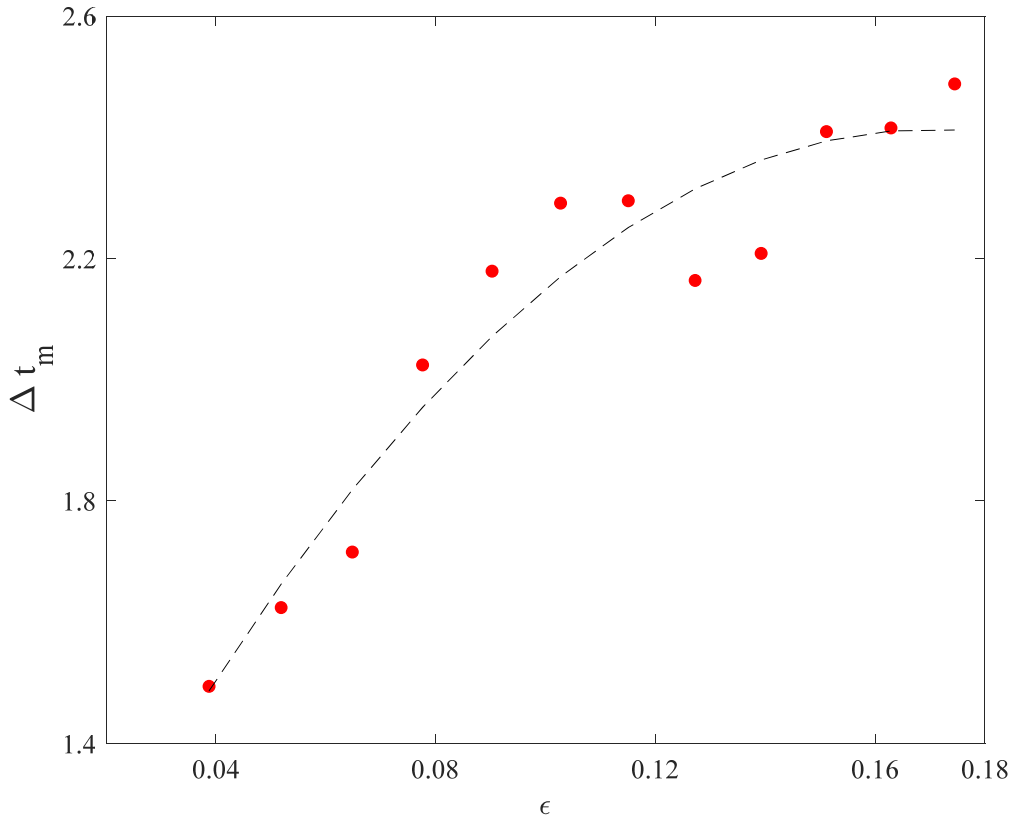

(a)

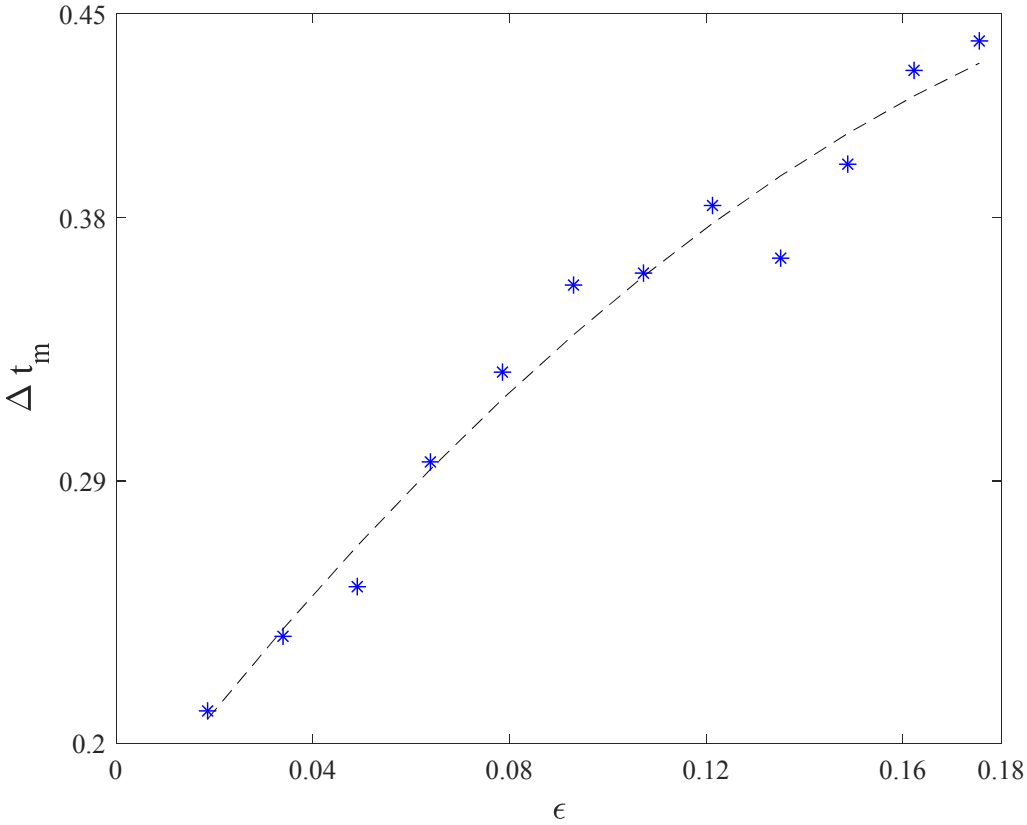

(b)

Figure III.8. Strain dependency of the average reloading time between two successive stress drops Δt_m at strain rates 2.38 10^{-4} s^{-1} (a) and 1.19 10^{-3} $s^{-}1$(b) in the Al-3.2%Mg alloy.

III.5.3. Stress drops distributions

A statistical analysis on stress drops is carried out in the Al -3.2% Mg alloy for two different applied strain rate: 2.38 10^{-4} s^{-1} and 1.19 10^{-3} s^{-1}. The results obtained are represented by the histograms in Figures III.9. The shape of the histograms depends on the applied strain rate. In the range of low strain rates (type B and C instabilities), the shape of the histograms is close to a Gaussian-type distribution indicating the random behavior of the plastic events (plastic localization). When the strain rate increases, the histogram becomes asymmetrical and shifts towards the small values of the stress drops. The appearance of PLC instabilities is therefore accompanied by the loss of symmetry of histograms when increasing the strain rate. This loss of symmetry is an indicator of the degree of spatial correlation between adjacent sections of the specimen [42].

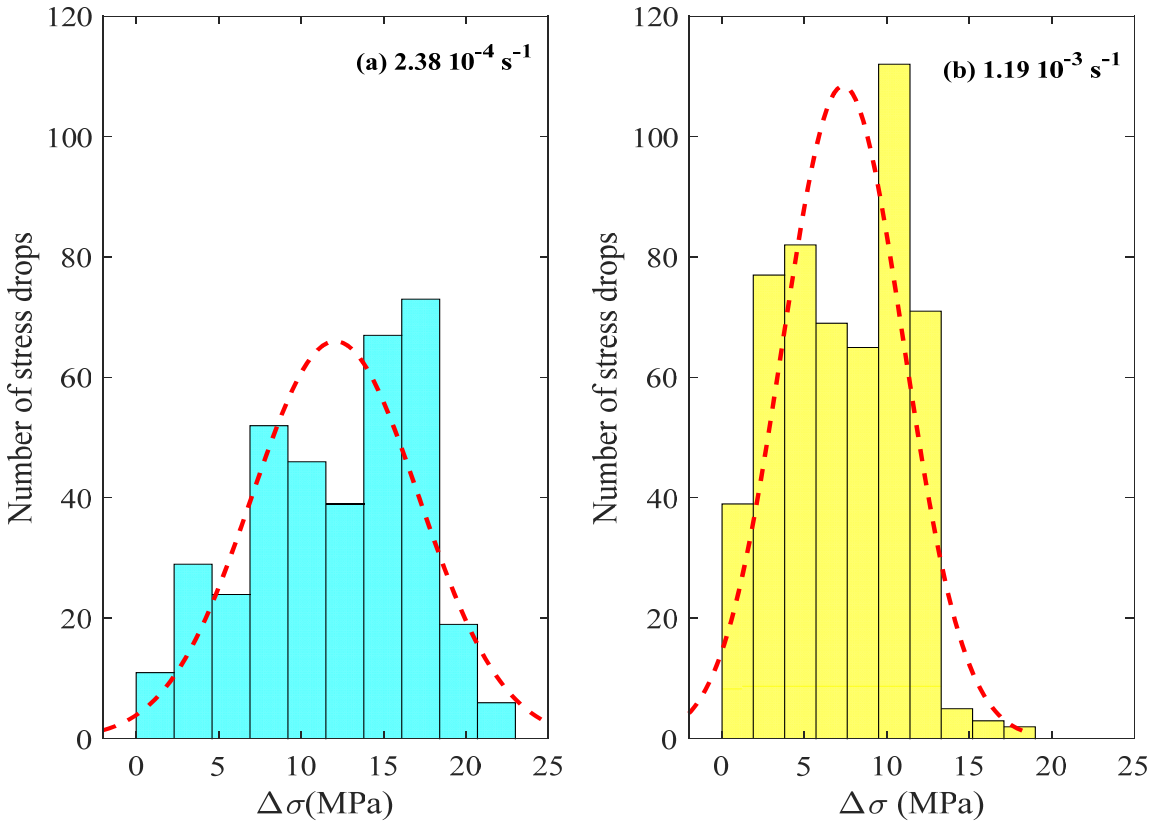

Figure III.9. Stress drops distributions at strain rates 2.38 10^{-4} s^{-1} (a) and 1.19 10^{-3} s^{-1}(b) in the Al-3.2%Mg alloy at room temperature.

III.6. Conclusion

Jerky flow and mechanical characteristics of the Al-3.2%Mg alloy are studied during tensile tests at room temperature. The experimental study highlights the influence of the imposed strain rate on mechanical behavior of the deformed material. Analysis of the tensile curves, at different strain rates, made it possible to determine the existence range of the PLC phenomenon and the different types of instabilities.

The critical plastic strain required for the appearance of jerky flow exhibits normal behavior at high strain rates, where instabilities are of type A, and inverse behavior at low strain rates, where the instabilities are of type C or B. Studying the evolution of plastic strain at fracture as a function of strain rate allowed us to show that the ductility of the Al-3.2%Mg alloy is affected by PLC instabilities. Evolution of the magnitude of the stress drops and the reloading time between successive instabilities showed that, due to DSA, they are of negative strain rate sensitivity.

Analysis of the statistical distributions of the stress drops has revealed a loss of their symmetry when the strain rate is increased. This shows that the transition from the random appearance of bands (type C) to the discontinuous mode (type B) and then to the continuous propagation mode (type A) is accompanied by an increase in spatial correlation of the plastic events occurring during deformation.

General conclusion

General conclusion

The mechanical behavior of a metallic material during plastic deformation is decisive for the success of the forming manufacturing process. For industrialists, who are increasingly using numerical simulation methods to develop and parameterize manufacturing processes through molding, a deep understanding of the intrinsic properties of materials is crucial.

In this work, we investigated the mechanical behavior of Al-Mg alloys during plastic deformation in order to gain a better understanding of their formability. These alloys, used for their good mechanical properties, have a major disadvantage: the appearance of the Portevin-Le Chatelier (PLC) phenomenon at room temperature. Under certain imposed conditions of strain rates, this phenomenon affects mechanical characteristics and leads to macroscopic heterogeneities.

By the end of the first chapter, we came to understand the different aspects of plastic deformation of crystalline metallic materials and the mechanisms associated with their microscopic scale. Thereafter, in the second part, we gave a phenomenological and analytical description of PLC instability by distinguishing it from heterogeneities of plastic deformation (spatial and temporal aspects). The characterization of the PLC effect in aluminum-magnesium alloys was carried out by the mechanical tensile test, in uniaxial conditions at constant imposed strain rates and at room temperature.

Jerky flow and mechanical characteristics of the Al-3.2%Mg alloy are studied at different applied strain rates and at room temperature. The experimental study highlights the influence of the strain and the imposed strain rate on mechanical behavior and the existence of a strain rates range of instability where jerky flow appear under different forms (spatial and temporal patterns). Evolution of the magnitude of the stress drops and the reloading time between successive instabilities showed that, due to DSA, they are of negative strain rate sensitivity.

Analysis of the statistical distributions of the stress drops has revealed a loss of their symmetry when the strain rate is increased. This shows that the transition from the random appearance of bands (type C) to the discontinuous displacement (type B) and then to the continuous propagation mode (type A) is accompanied by an increase in spatial correlation of the plastic events occurring during deformation.

References

References

[1] C. Kittel, *Introduction to Solid State Physics*, J. Wiley& Sons Inc, 8th Edition, 2005.

[2] M. Ladd, *Crystal structures lattices and Solids in Stereo view*, Wood head publishing, 1999.

[3] A. Kelly and K.M. Knowles, *Crystallography and Crystal Defects*, Published by John Wiley & Sons, Ltd. 2nd Edition, 2012.

[4] H. Ait-Amokhtar, *Microstructures et propriétés des matériaux*, Cours M1 Physique des matériaux, Université de Bejaia, 2020/2021.

[5] J.P. Mercier, G. Zambelli and W. Kurz, *Introduction à la science des matériaux*, Presses Polytechniques et universitaires romandes, 3ème édition, 2002.

[6] J.C.Charmet, *Mécanique du solide et des matériaux. Elasticité-Plasticité-rupture*, ESPCI, Presses universitaires, 2005.

[7] T.-T. Fang, *in Elements of Structures and Defects of Crystalline Materials*, 2018

[8] D. Hull and D. J. Bacon, *Introduction to Dislocations*, Published by Elsevier Ltd. 5th Edition, 2011.

[9] G. Daveau, Thèse de Doctorat, Ecole Centrale Paris,(2012).

[10] K. G. Bøving, *Non-Destructive Examination Methods for Condition,* Monitoring NDT & E International (1989) 103.

[11] N. Saba, M.T.H. Sultan, *in Mechanical and Physical Testing of Biocomposites, Fibre-Reinforced Composites and Hybrid Composites*, 2019.

[12] T. W. Clyne and J. E. Campbell, *Testing of the Plastic Deformation of Metals*, Cambridge University Press, 2021.

[13] C.K. Chua, W. Y. Yeong, *in Standards, Quality Control, and Measurement Sciences in 3D Printing and Additive Manufacturing*, 2017.

[14] H. Farhat, *in Operation, Maintenance, and Repair of Land-Based Gas Turbines*, 2021

[15] V. Koncar, *Smart Textiles for In Situ Monitoring of Composites*, 1st edition, The Textile Institute Book Series 2019.

[16] J. R. Davis, Tensile Testing, ASM International, Second Edition 2004.

[17] Y. Estrin, L.P. Kubin, Acta metal. Vol.38, No 5 (1990) 697.

[18] M.F. Ashby and D.R. H. Jones, Y. Brechet, *Matériaux 1., Propriétés, applications et conception*,3rd Edition, 2008.

[19] Y. Estrin, L. P. Kubin, Mater. Sci. Eng. A 137 (1991) 125.

[20] A. Luft, *Progress in Materials Science*35 (1991) 97.

[21] K. Bouabdallah, Thèse de Doctorat, Université de Sétif, (2007).

[22] M.G. Darieulat et J.H.Driver, Rev. De Met.-CIT/Sci. et Génie de Mat. (1997)1011.

[23] G.G. Saha, P.G. McCormick and P. Ramarao, Mater. Sci. Eng. A 62, (1984) 187.

[24] A. Zeghloul, M. Mliha-Touati et S. Bakir, *Étude des domaines d'existence des instabilités plastiques du type Portevin-Le Chatelier dans l'alliage d'aluminium-magnesium AG3*J. Phys. III France 6 (1996) 1467-1478.

[25] E.Pink, A.Grinberg, *Stress drops in serrated flow curves of Al-5Mg,* Acta Met.30 (1982) 2153.

[26] J. Balik, P. Lukac and L.P. Kubin, Scripta Mat. 42 (2000) 465.

[27] K. Chihab, Thèse de Doctorat, Univ. de Poitiers, (1986).

[28] P. Kubin, K. Chihab and Y. Estrin, NATO ASI Series E, App. Sci. 121, (1987) 220.

[29] R.W.K. Honeycombe, *The plastique deformation of metals*, Ed. Edward Arnolds, (1977).

[30] J. M.Dorlot, J. P.Baillon, J. Masonnave, *Des matériaux*, Ed. Ecole polytechnique de Montréal, (1986).

[31] A. Van den Beukel, Phys. Stat. Sol. (a), Vol.30 (1975) 197.

[32] L.J. Cuddy, W.C. Leslie, Acta Metall.20 (1972) 1157.

[33] U.F. Kocks, *Progress in Materials Science*, Chalmers Anniversary Volume, Pergamon press (Oxford) (1981)185.

[34] J. Caisso, J. Guillot, Mem. Sc. Rev. Metall. 5 (1962)395.

[35] H. Ait-Amokhtar, Thèse de Doctorat, Université de Béjaia, (2006).

[36] D. François, A. Pineau et A. Zaoui, *Comportement mécanique des matériaux,* HERMES, (1991)

[37] H. Mughrabi, *Plastic Deformation and Fracture of Materials,* Materials Science and Technology, Vol.6 Edited byR.W. Cahn, P. Haasen, E.J. Kramer(1996).

[38] J.P. Baïlon, J.M. Dorlot, *Des Matariaux,*J.P. Baïlon, Presses Internationales de Polytechnique, 3ème Edition,

[39] N. Chibane, H. Ait-Amokhtar, 21èmeCongrès Français de Mécanique, Bordeaux, 26 au 30 août 2013.

[40] H. Ait-Amokhtar, C. Fressengeas, K. Bouabdallah, Mater. Sci. Eng.A 631 (2015) 209.

[41] P.G. McCormick, Acta Metall. 20 (1972) 351.

[42] M. Mehenni, H. Ait-Amokhtar, C. Fressengeas, Mater. Sci. Eng. A 756 (2019) 313.

Analysis of stress drops associated with the heterogeneous plastic deformation in the Al-3.2%Mg alloy

Abstract

Aluminum alloys have a wide range of applications due to their interesting properties. They are used in many and different applications, particularly in corrosive environments. During plastic deformation of Al-Mg alloys, the magnesium can diffuse and interact with mobile dislocations. Under certain conditions, this dynamic interaction leads to strain localizations of Portevin-Le Chatelier (PLC) type.

In the present work, jerky flow and mechanical characteristics of the Al-3.2%Mg alloy were studied during tensile tests at room temperature. The study highlights the effect of the imposed strain and strain rate on the mechanical behavior of the studied material and on the associated patterns of plastic instabilities. Under the imposed deformation conditions, it is shown that the transition from the random appearance of bands (type C) to the discontinuous mode (type B) and then to the continuous propagation mode (type A) is accompanied by an increase in spatial correlation of the plastic events occurring during plastic deformation.

Keywords: Al-Mg alloys; Dislocations; Dynamic strain aging; Portevin–Le Chatelier effect; Strain localizations.

Analyse des chutes de contraintes associées à la déformation plastique hétérogène dans l'alliage Al-3.2%Mg

Résumé

Les alliages d'aluminium ont une large gamme d'applications en raison de leurs propriétés intéressantes. Ils sont utilisés dans de nombreuses et différentes applications, en particulier dans les environnements corrosifs. Pendant la déformation plastique des alliages Al-Mg, le magnésium peut diffuser et interagir avec les dislocations mobiles. Sous certaines conditions, cette interaction dynamique conduit à des localisations de la déformation de type Portevin-Le Chatelier (PLC).

Dans le présent travail, l'écoulement plastique instable et les caractéristiques mécaniques de l'alliage Al-3,2%Mg ont été étudiés lors d'essais de traction à température ambiante. L'étude met en évidence l'influence de la déformation et de la vitesse de déformation imposées sur le comportement mécanique du matériau étudié et sur les motifs d'instabilités associés. Dans les conditions de déformation imposées, on montre que le passage de l'apparition aléatoire des bandes (type C) au mode discontinu (type B) puis au mode de propagation continue (type A) s'accompagne d'une augmentation de la corrélation spatiale des événements plastiques se produisant au cours de la déformation plastique.

Mots-clés: Alliages Al-Mg; Dislocations; Vieillissement dynamique; Effet Portevin-Le Chatelier ; Localisations de la déformation.